Cold nuclear matter effects on heavy quark production

Kirill Tuchin

IOWA STATE UNIVERSITY
OF SCIENCE AND TECHNOLOGY

Forward Physics at RHIC workshop, BNL, July-August 2012

Heavy quarks: motivation

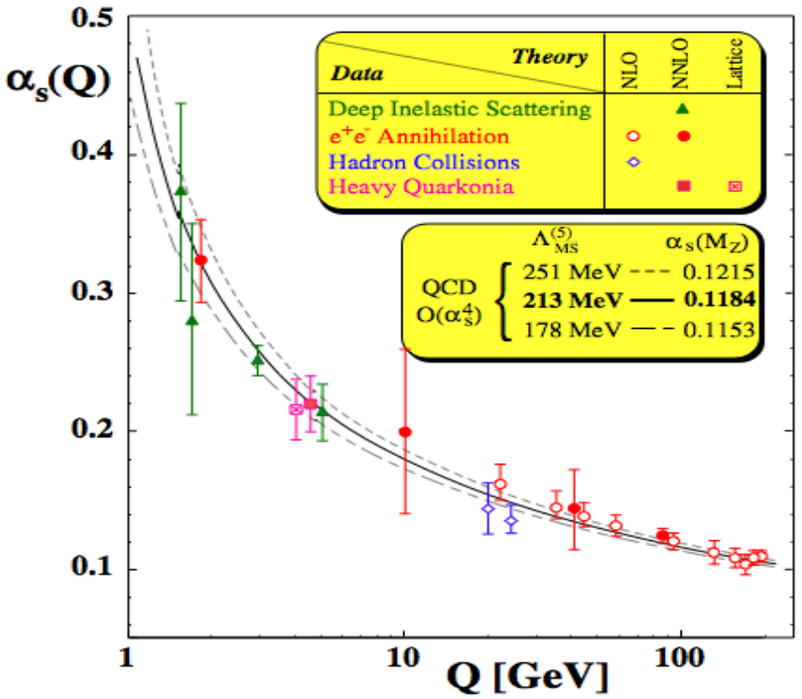

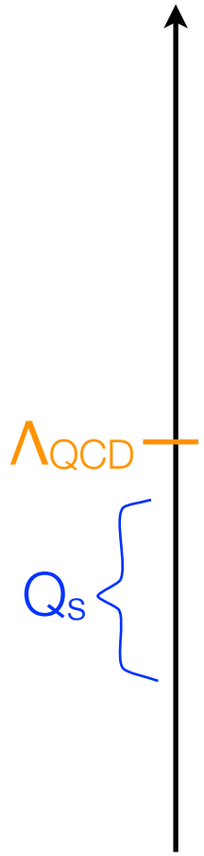

Flavor	Mass	
u	$1.5 - 4.5$ MeV	Light quarks
d	$5.0 - 8.5$ MeV	
s	$80 - 155$ MeV	
c	$1.0 - 1.4$ GeV	Heavy quarks
b	$4.0 - 4.5$ GeV	
t	174.3 ± 5.1 GeV	

Heavy quarks have masses that are much larger than the typical QCD scale Λ_{QCD}

Asymptotic freedom: $\alpha_s(m^2) \ll 1$ Perturbation theory is applicable!

Higher twist effects ~ $\dfrac{\langle \alpha_s G^2 \rangle}{m^4} \ll 1$ $\dfrac{Q_s^2}{m^2}$

J/ψ in hot medium

Immersing J/ψ in quark-gluon plasma modifies

- J/ψ binding potential V(r,T)
- J/ψ wave function Φ(r,T),
- J/ψ formation rate $\propto |\Phi(r,T)|^2$,

and turns on new production mechanisms such as recombination etc.

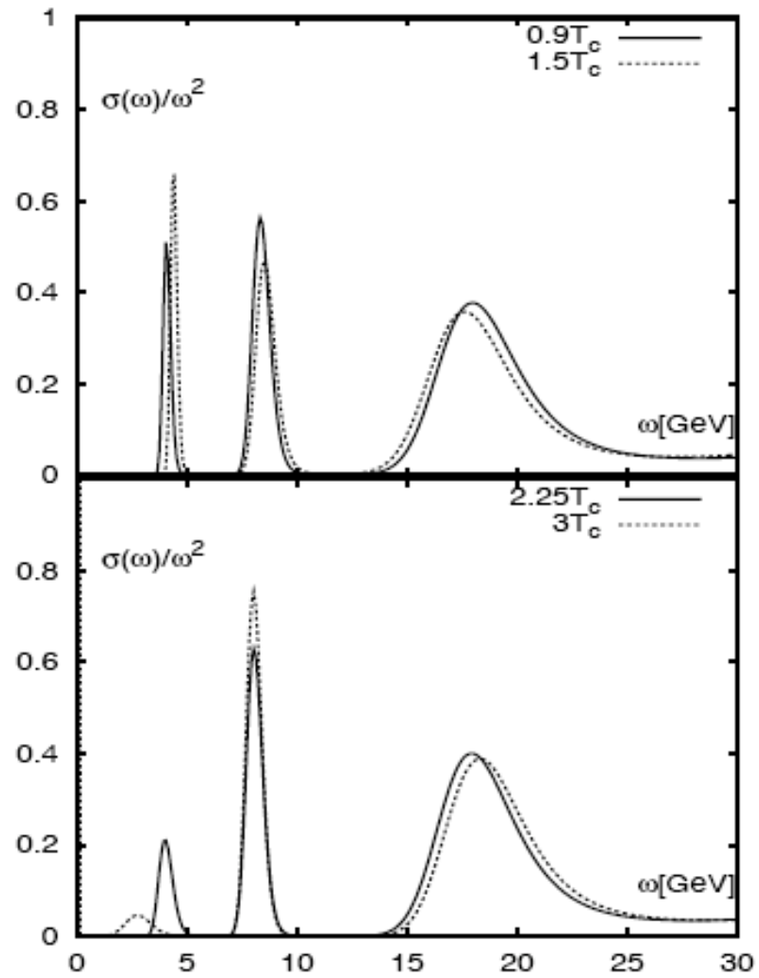

If we have a good theoretical control of these processes we will be able to extract medium properties from the J/ψ production cross sections.

First, we need to understand J/ψ production in pp and in pA collisions.

Factorization ?

HARD PQCD:

Factorization → Universal pdf's → Phenomenology

- Factorization is broken if the hard amplitude involves *simultaneous* interactions with more than two partons at a time.

- Coherent scattering: $l_c >> R_A$ (coherence effects start at $l_c \sim R_p$)

CGC/saturation = implementing the coherence.

Assuming factorization...

The effective absorption cross sections from fits of Ramona's calculations to PHENIX d+Au R_{CP} data are shown for each shadowing model.

This is **not** an attempt to extract physics from the d+Au R_{CP}! This is just a parameterization of the data that is independent at each rapidity.

The red points are the averages at y = -1.7 and +1.7.

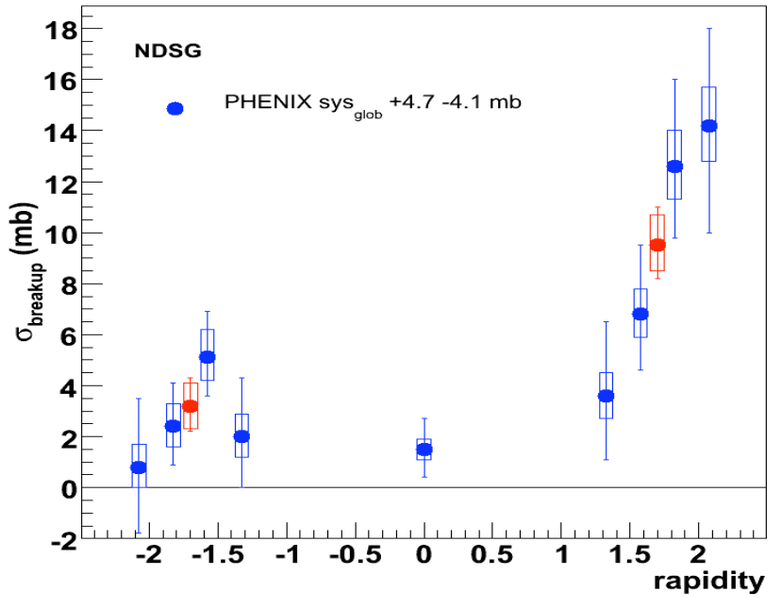

Slide stolen from T. Frawley

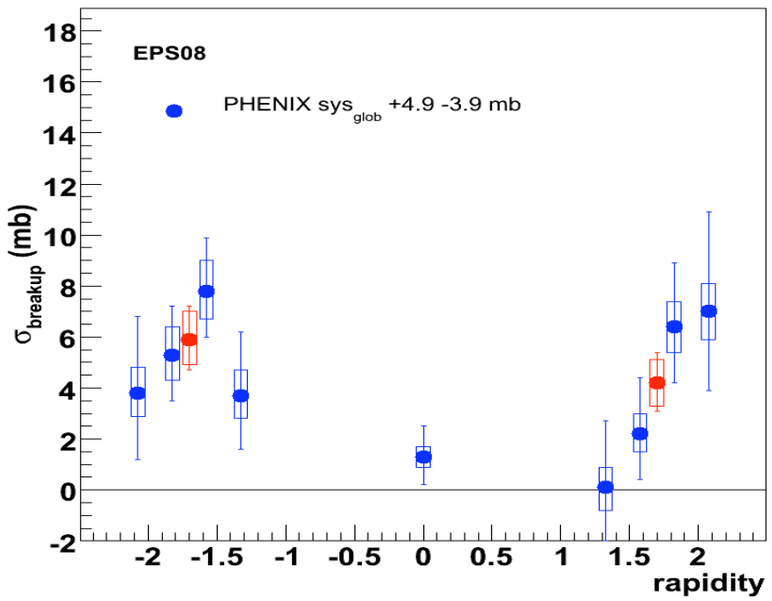

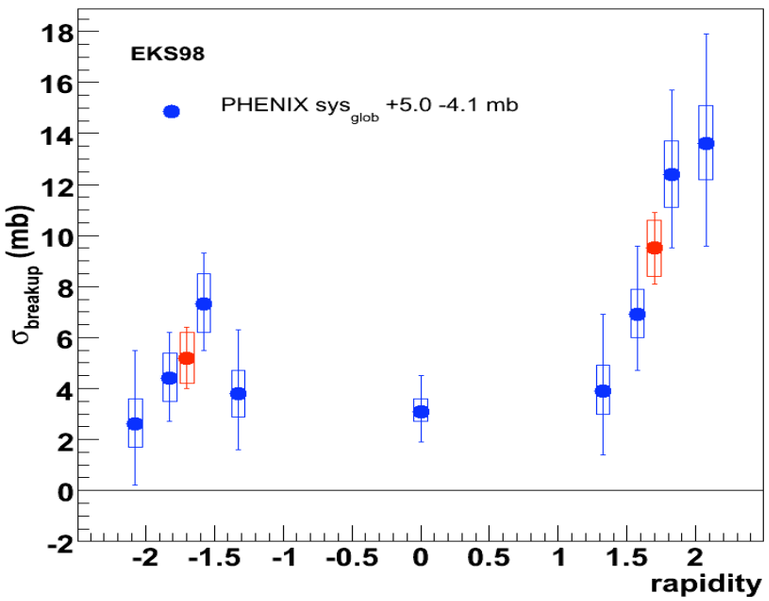

This does not look like a reasonable behavior.

Coherence

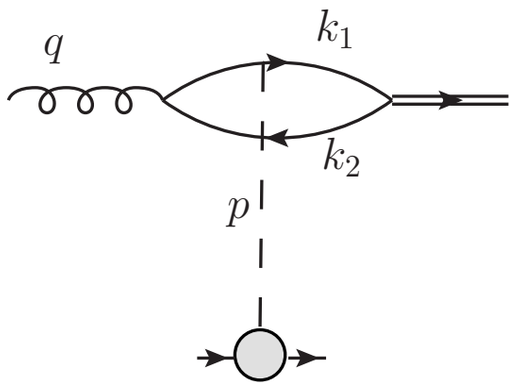

Longitudinal momentum transfer

$$p_z = q_z - k_{1z} - k_{2z} \approx \frac{\boldsymbol{k}_1^2 + m^2}{2z\omega} + \frac{(\boldsymbol{p} - \boldsymbol{k}_1)^2 + m^2}{2(1-z)\omega}$$

$$|\boldsymbol{k}_1 - \boldsymbol{k}_2| \sim \alpha_s m \ll p_\perp \qquad z \approx 1/2$$

$$p_z = \frac{1}{\omega}\left[p_\perp^2 + (2m)^2\right] = \frac{2}{\sqrt{s}} e^{-y}\left[p_\perp^2 + (2m)^2\right]$$

The *longitudinal form factor* is a measure of the coherence of high energy process

$$\mathcal{F}_L(p_z) = \frac{1}{A}\int d^2b \int_{-\infty}^{\infty} d\xi\, \rho(\boldsymbol{b},\xi)\, e^{ip_z\xi}$$

Coherent scattering: $l_c \sim \dfrac{1}{p_z} > R_A$ ☞ $\mathcal{F}_L \approx 1$

The longitudinal form factor

For the “hard sphere” nucleus

$$\mathcal{F}_L = \frac{3}{(p_z R_A)^3}\left[\sin(p_z R_A) - p_z R_A \cos(p_z R_A)\right]$$

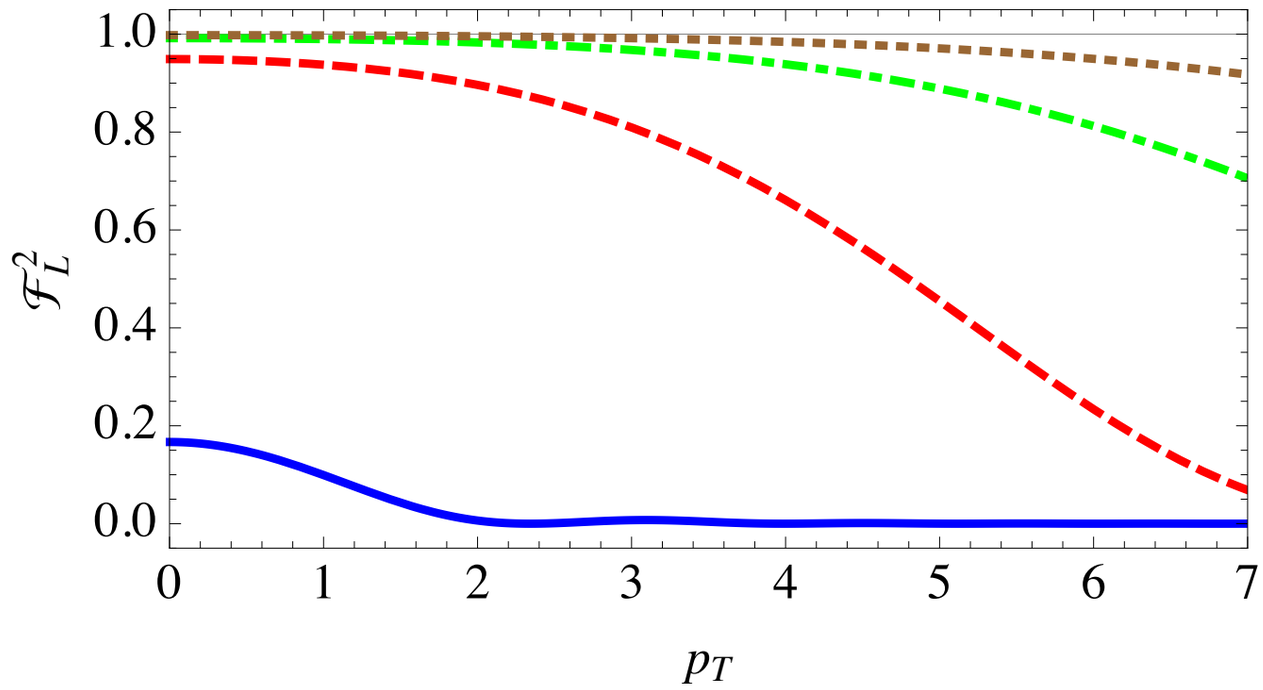

FIG. 8: (Color online). Square of the longitudinal form factor as a function of transverse momentum of J/ψ in GeV's. Lines from bottom to top: $\sqrt{s} = 0.2$ TeV, $y = 0$ (blue, solid), $\sqrt{s} = 0.2$ TeV, $y = 1.7$ (red, dashed), $\sqrt{s} = 2.76$ TeV, $y = 0$ (green, dot-dashed), $\sqrt{s} = 5.5$ TeV, $y = 0$ (brown dashed).

The time scales

A pre-hadron cc pair is produced over time

$$\tau_P = l_c/c = 7\, e^y \,\mathrm{fm}$$

J/ψ wave function is formed over time

$$\tau_F = \frac{2\, M_\psi}{M_{\psi'} - M_\psi} l_c = 42\, e^y \,\mathrm{fm}$$

Hierarchy of scales required for the dipole model: $\tau_F >> \tau_P >> \tau_{INT}$

J/ψ production mechanisms in pp

Baier Ruckl, 1981

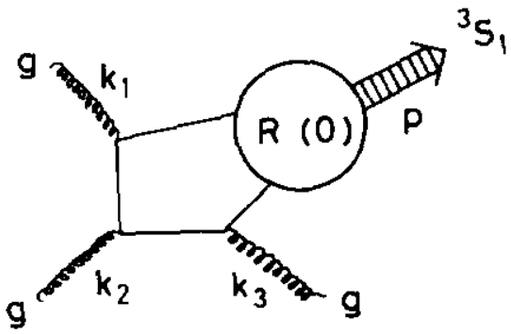

- Color singlet model

$q\bar{q}$ must have the same quantum numbers as the final quarkonia.

The wave function parameter ψ(0) is uniquely fixed using the J/ψ decay rate.

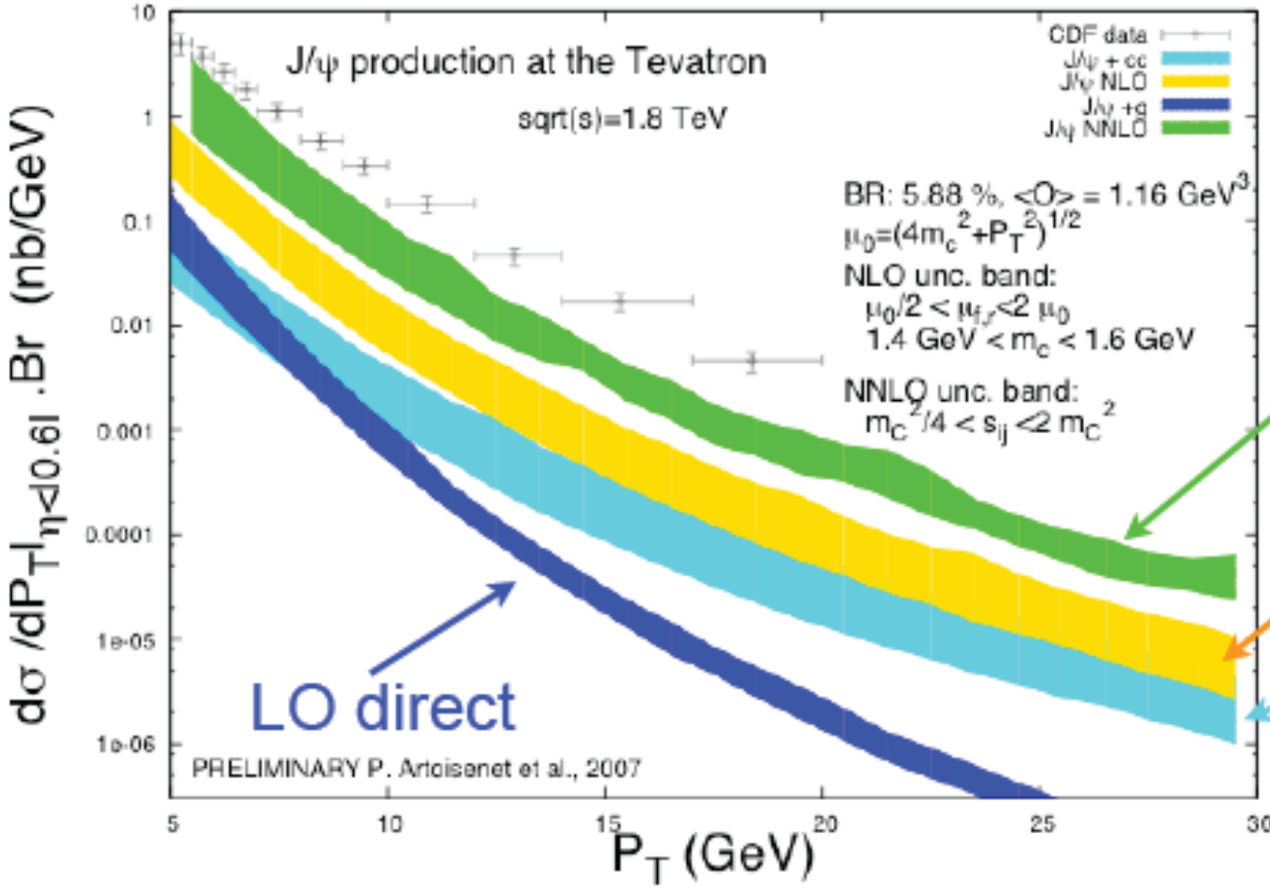

Artoisenet, Landsberg, Maltoni, 2007

- Far from data
- Strong scale dependance
- Poor convergence

NNLO

NLO

LO associate

J/ψ production mechanisms in pp (cont.)

- Non-relativistic QCD model

  Gives the best fit to Tevatron p_T spectra, but has a lot of free parameters (non-perturbative matrix elements).

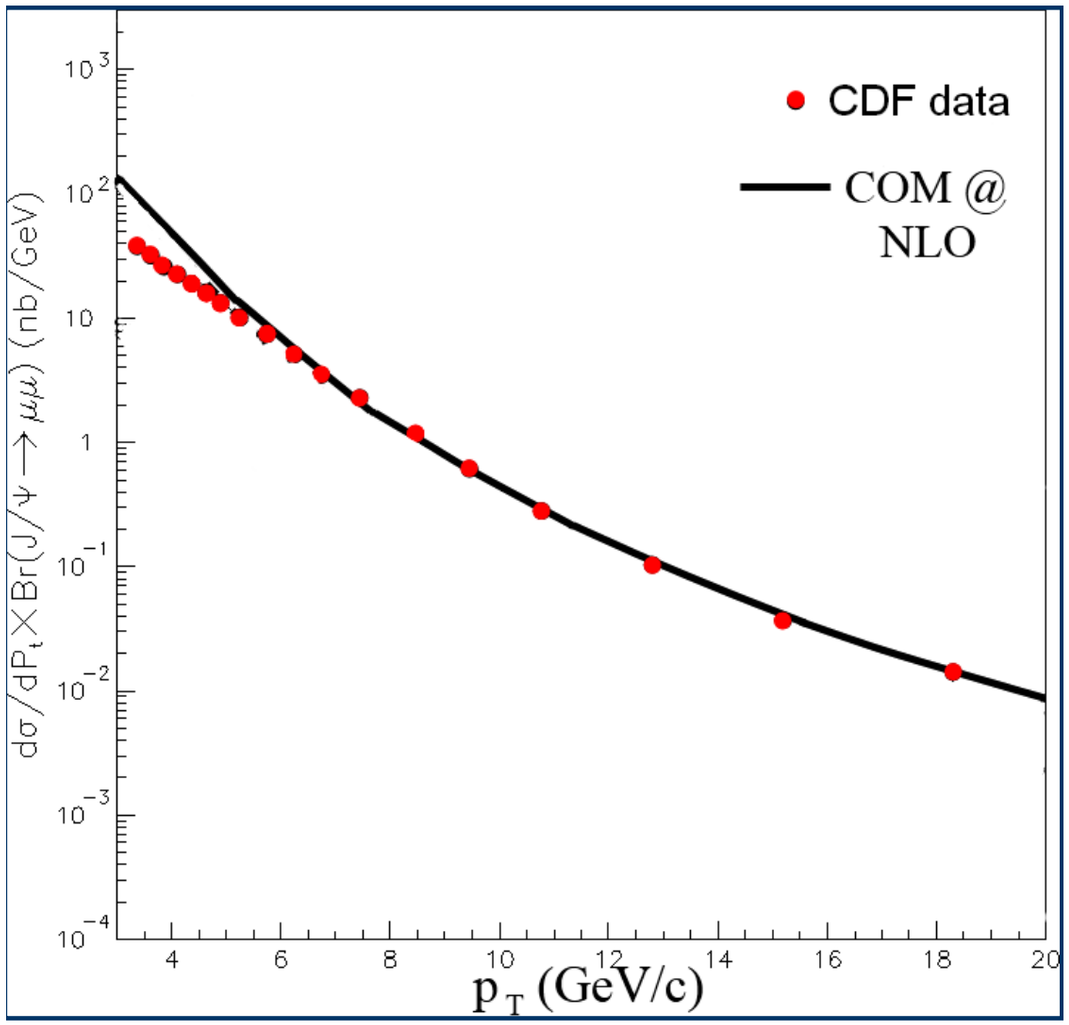

- Misses polarization.
- Fails for associated production

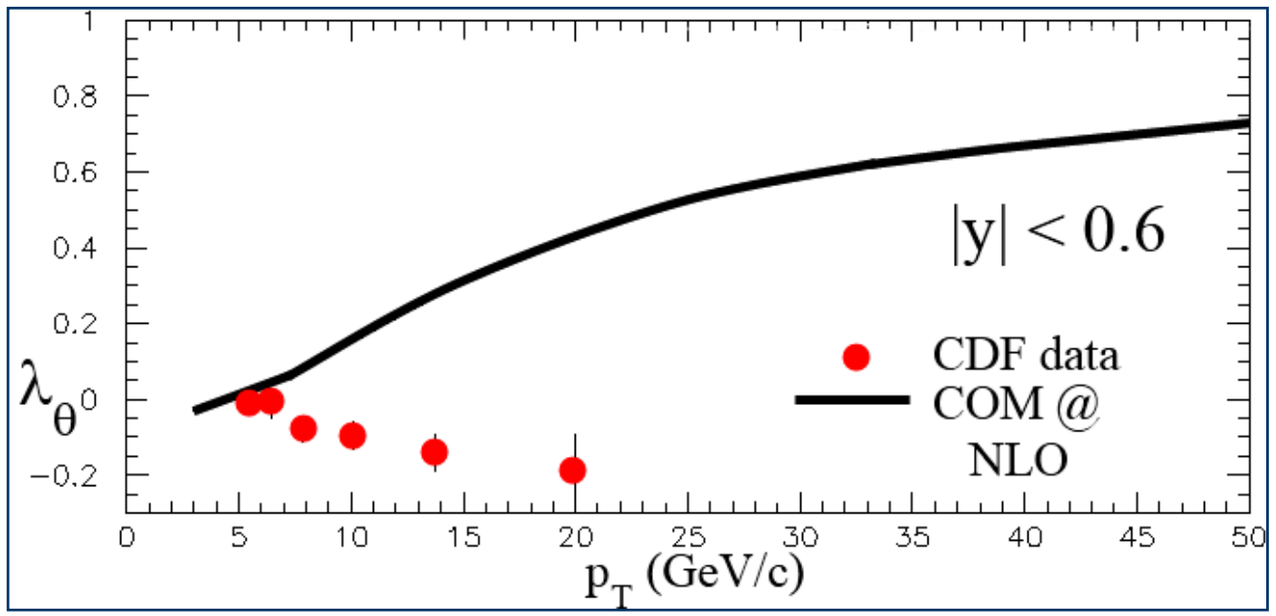

J/ψ production mechanisms (cont.)

Higher twist effects must be properly taken into account

Qiu, Sterman

Do we have a chance to understand the J/ψ production in pA and AA if we don't fully understand it in pp?

Possibly yes, because we have an additional parameter A>>1 that allows to re-sum parametrically large higher twists contributions.

Production of J/ψ: pp vs pA

Kharzeev, KT (2005)

Kharzeev, Levin, KT (2008)

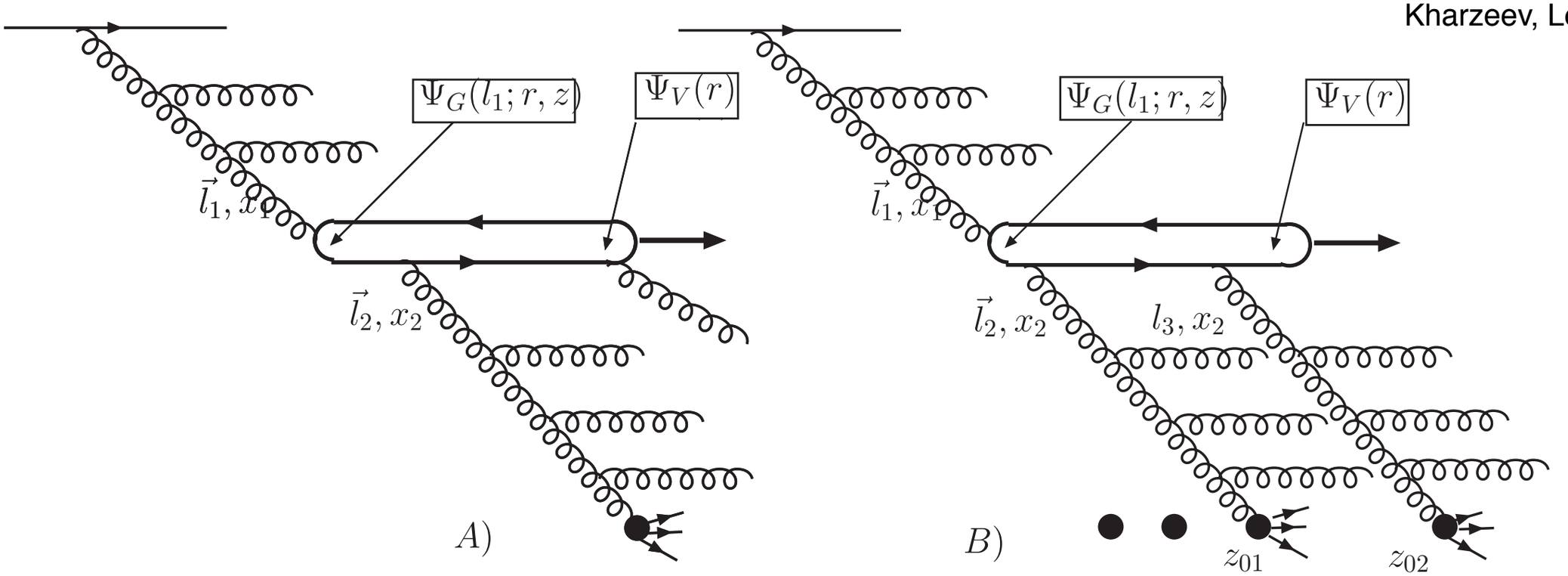

$hadron - hadron \quad collisions$

$$\alpha_s^3 A^{1/3} = \alpha_s \underbrace{(\alpha_s^2 A^{1/3})}_{\alpha_s^2 A^{1/3} \sim 1} \sim \alpha_s$$

$hadron - nucleus \quad collisions$

$$\alpha_s^4 A^{2/3} = (\alpha_s^2 A^{1/3})^2 \sim 1$$

This diagram breaks factorization.

Quasi-classical approximation

Dominguez, Kharzeev, Levin, Mueller, KT (2011)

Kharzeev, Levin, KT (2012)

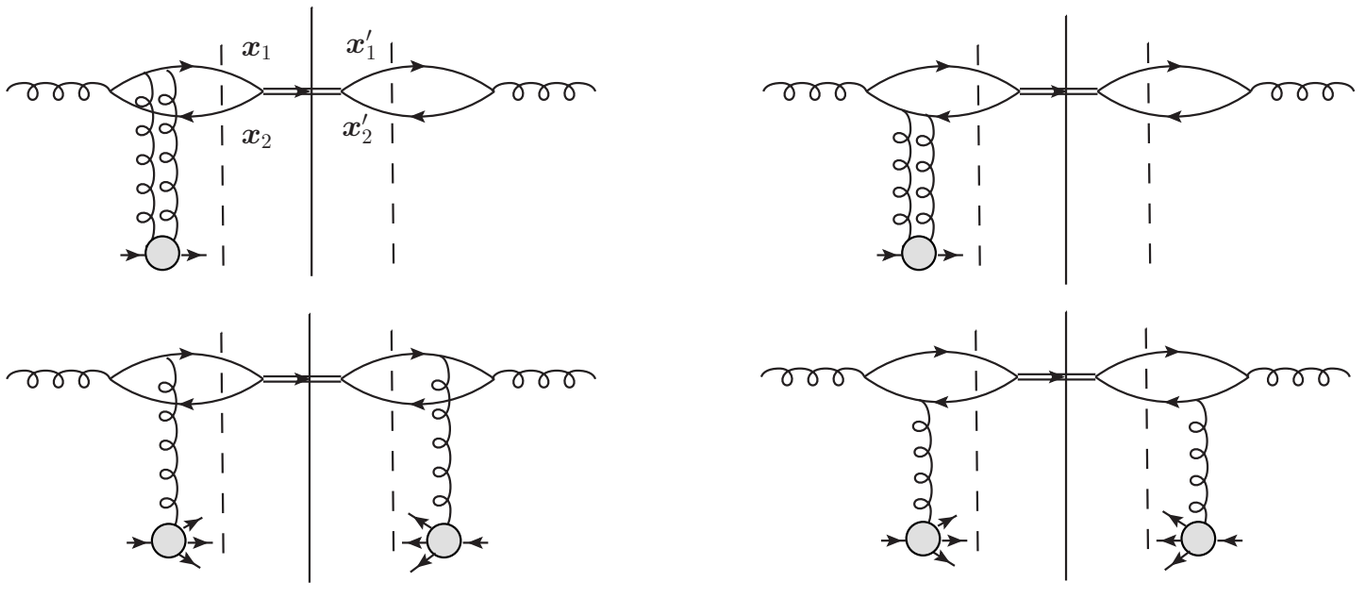

$$\boldsymbol{x}_1 = \boldsymbol{b} + \frac{1}{2}\boldsymbol{r}\,, \quad \boldsymbol{x}_2 = \boldsymbol{b} - \frac{1}{2}\boldsymbol{r}\,,$$

$$\boldsymbol{x}_1' = \boldsymbol{b}' + \frac{1}{2}\boldsymbol{r}'\,, \quad \boldsymbol{x}_2' = \boldsymbol{b}' - \frac{1}{2}\boldsymbol{r}'\,,$$

$$\boldsymbol{\Delta} = \boldsymbol{b} - \boldsymbol{b}'\,, \quad \boldsymbol{B} = \frac{1}{2}(\boldsymbol{b} + \boldsymbol{b}')$$

FIG. 1: One of the interactions before the last inelastic scattering. The diagrams that are complex conjugate to the first row of diagrams are not shown. The vertical dashed line denotes the last inelastic interaction when the $c\bar{c}$ pair is converted into the color-singlet state. The vertical solid line is the cut corresponding to the final state.

$$-\frac{1}{8}Q_s^2(B)\left[(\boldsymbol{x}_1 - \boldsymbol{x}_1')^2 + (\boldsymbol{x}_2 - \boldsymbol{x}_2')^2\right] = -\frac{1}{4}Q_s^2(B)\left(\Delta^2 + \frac{1}{4}(\boldsymbol{r} - \boldsymbol{r}')^2\right)$$

modulo log's (dropping logs: GBW model/geometric scaling)

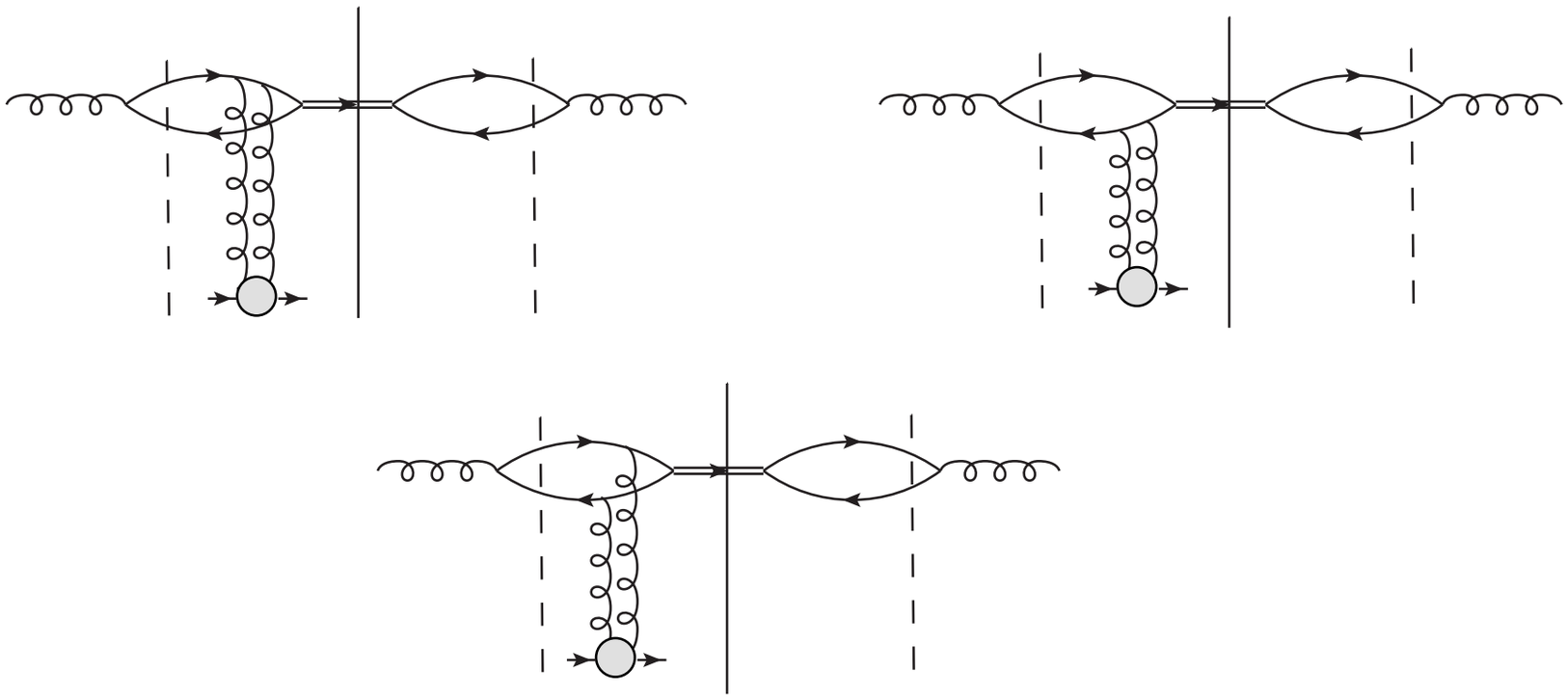

FIG. 2: One of the interactions after the last inelastic interactions. Complex conjugate diagrams are not shown.

$$-\frac{1}{8}Q_s^2(B)\left[(\boldsymbol{x}_1-\boldsymbol{x}_2)^2+(\boldsymbol{x}_1'-\boldsymbol{x}_2')^2\right]=-\frac{1}{8}Q_s^2(B)(r^2+r'^2)$$

modulo log's

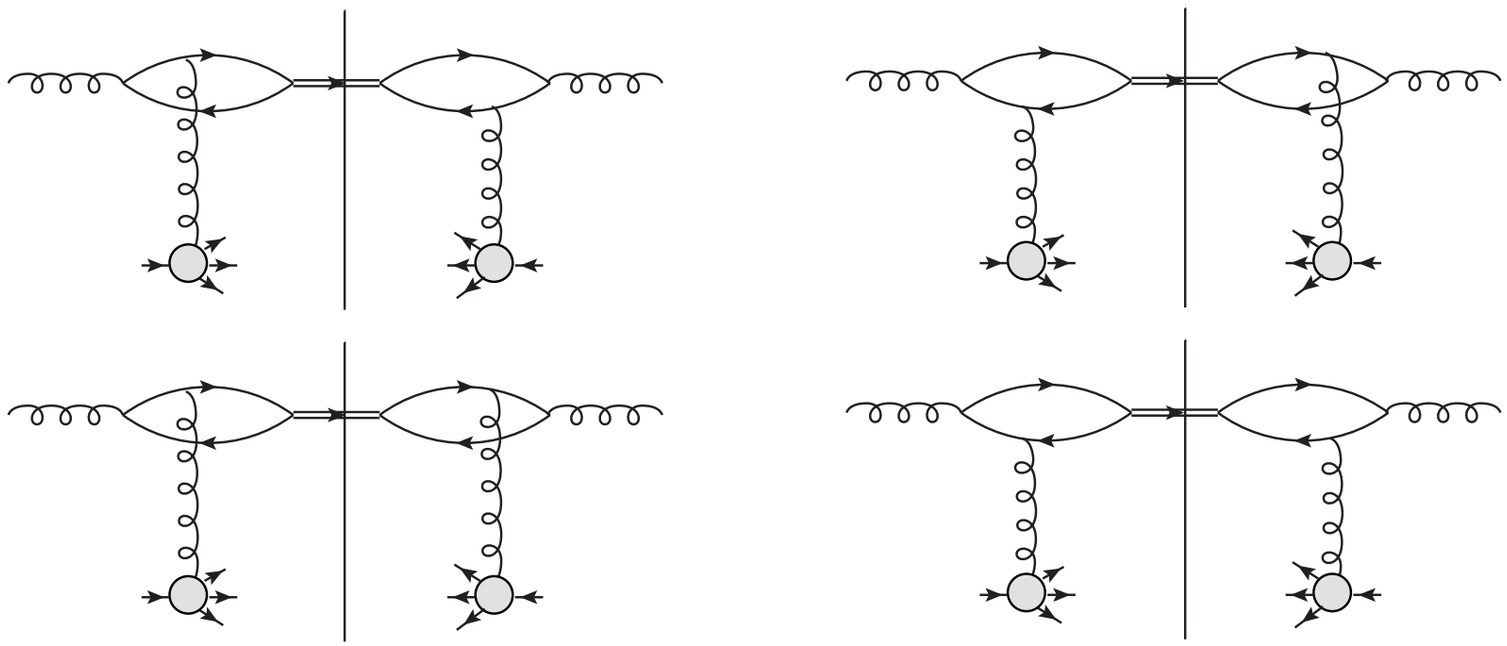

FIG. 3: The last inelastic interaction.

$$-\frac{1}{8}Q_s^2(B)\left[(\boldsymbol{x}_2-\boldsymbol{x}_1')^2+(\boldsymbol{x}_1-\boldsymbol{x}_2')^2-(\boldsymbol{x}_1-\boldsymbol{x}_1')^2-(\boldsymbol{x}_2-\boldsymbol{x}_2')^2\right]=-\frac{1}{4}Q_s^2(B)\,\boldsymbol{r}\cdot\boldsymbol{r}'$$

modulo log's

Amplitude for J/ψ production $\quad A(p_\perp) = \dfrac{1}{p_\perp^2}\mathcal{F}(p_\perp)$ with the form-factor:

$$\mathcal{F}(p_\perp) = \int \frac{d^3k}{(2\pi)^3}\Psi_G(k)\,\Psi_V(k-p) = 2\pi\alpha_s \int_0^1 dz \int \frac{d^2r}{4\pi}\Phi(r,z)\left(e^{-i\frac{1}{2}\boldsymbol{r}\cdot\boldsymbol{p}} - e^{i\frac{1}{2}\boldsymbol{r}\cdot\boldsymbol{p}}\right)$$

g→J/ψ transition amplitude squared

$$\Phi(\boldsymbol{r},z) = \frac{g}{\pi\sqrt{2N_c}}\left\{m_c^2 K_0(m_c r)\phi_T(r,z) - \left[z^2+(1-z)^2\right] m_c K_1(m_c r)\partial_r\phi_T(r,z)\right\}$$

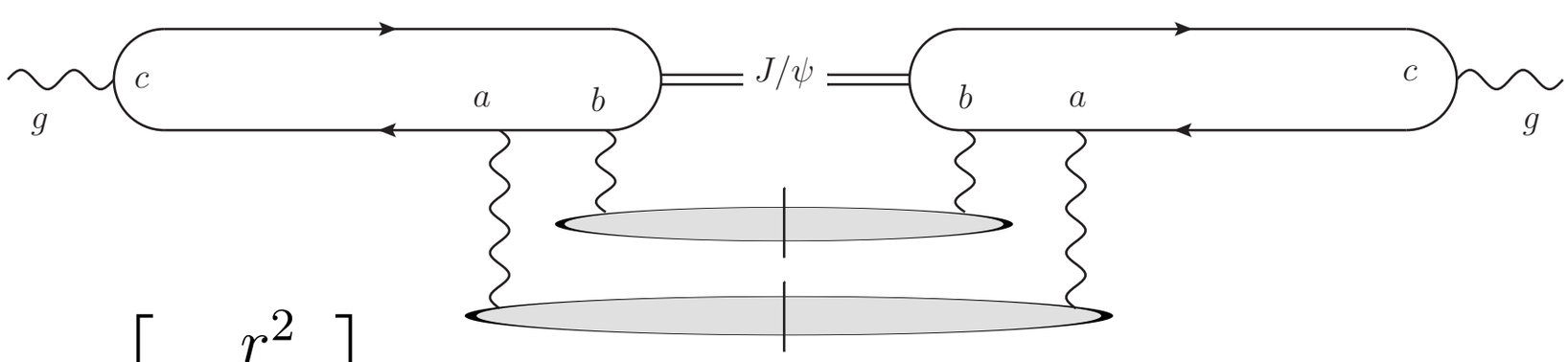

J/ψ wave function

$$\phi_T(r,z) = N_T z(1-z)\exp\left[-\frac{r^2}{2R_T^2}\right]$$

N_T, R_T are fixed from DIS

Total inclusive cross section

Sum over multiple scatterings, integrate over p_T and over the longitudinal coordinate of the last inelastic interaction ξ

$$\frac{d\sigma_{gA\to J/\psi X}}{d^2b} = \int_0^1 dz \int \frac{d^2r}{4\pi}\Phi(\boldsymbol{r},z)\int_0^1 dz' \int \frac{d^2r'}{4\pi}\Phi^*(\boldsymbol{r'},z')$$
$$\times \int_0^{T(b)} d\xi\, \frac{\boldsymbol{r}\cdot\boldsymbol{r'}Q_s^2}{4T(b)} \exp\left\{-\frac{1}{16}Q_s^2(\boldsymbol{r}-\boldsymbol{r'})^2\frac{\xi}{T(b)} - \frac{1}{8}Q_s^2(r^2+r'^2)\left(1-\frac{\xi}{T(b)}\right)\right\}$$

☞ $$\frac{d\sigma_{pA\to J/\psi X}}{dyd^2b} = x_1 G(x_1,m_c^2)\int_0^1 dz \int \frac{d^2r}{4\pi}\Phi(\boldsymbol{r},z)\int_0^1 dz' \int \frac{d^2r'}{4\pi}\Phi^*(\boldsymbol{r'},z')$$
$$\times \frac{4\boldsymbol{r}\cdot\boldsymbol{r'}}{(\boldsymbol{r}+\boldsymbol{r'})^2}\left(e^{-\frac{Q_s^2}{16}(\boldsymbol{r}-\boldsymbol{r'})^2} - e^{-\frac{Q_s^2}{8}(r^2+r'^2)}\right)$$

From pA to AA

Now c-dipole can scatter in both nuclei ⇒ need to account for the nuclear matter distribution in another nucleus

$$\frac{\alpha_s \pi^2}{4C_F} x_1 G(x_1, a^2) = \int d^2 b_1 \, \frac{Q_{s1}^2}{8}$$

Kovchegov (2001)

$$\frac{d\sigma_{A_1 A_2 \to J/\psi X}}{dy \, d^2b \, d^2B} = \int_0^1 dz \int \frac{d^2\boldsymbol{r}}{4\pi} \int_0^1 dz' \int \frac{d^2\boldsymbol{r}'}{4\pi} \, \Phi(\boldsymbol{r}, z) \, \Phi^*(\boldsymbol{r}', z') \, 2T_{A_1 A_2 \to JX}(\boldsymbol{r}, \boldsymbol{r}')$$

$$T_{A_1 A_2 \to JX}(\boldsymbol{r}, \boldsymbol{r}') = \frac{C_F}{2\alpha_s \pi^2} \frac{Q_{s1}^2 Q_{s2}^2}{Q_{s1}^2 + Q_{s2}^2} \frac{4\boldsymbol{r} \cdot \boldsymbol{r}'}{(\boldsymbol{r} + \boldsymbol{r}')^2} \left(e^{-\frac{1}{16}(Q_{s1}^2 + Q_{s2}^2)(\boldsymbol{r} - \boldsymbol{r}')^2} - e^{-\frac{1}{8}(Q_{s1}^2 + Q_{s2}^2)(r^2 + r'^2)} \right)$$

At small r: $T_{A_1 A_2 \to JX}(\boldsymbol{r}, \boldsymbol{r}') \approx \frac{C_F}{2\alpha_s \pi^2} Q_{s1}^2 Q_{s2}^2 \, 4\boldsymbol{r} \cdot \boldsymbol{r}' \left(\frac{1}{16} - \frac{1}{512}(Q_{s1}^2 + Q_{s2}^2)(3r^2 + 3r'^2 - 2\boldsymbol{r} \cdot \boldsymbol{r}') \right)$

Averaging over angles: $\left\langle T_{A_1 A_2 \to JX}(\boldsymbol{r}, \boldsymbol{r}') \right\rangle \approx \frac{C_F}{\alpha_s \pi^2} \frac{r^2 r'^2}{16^2} \, (Q_{s1}^2 Q_{s2}^4 + Q_{s1}^4 Q_{s2}^2)$

3 scatterings

Low x evolution

The low x evolution gives energy/rapidity dependence

Glauber-Mueller formula for quark dipole scattering is the initial condition

$$N_F(\boldsymbol{r}, \boldsymbol{b}, y_0) = 1 - e^{-\frac{1}{8}\boldsymbol{r}^2 Q_s^2(y_0)}$$

Amplitude for gluon (adjoint) dipole:

$$N_A(\boldsymbol{r}, \boldsymbol{b}, y) = 2N_F(\boldsymbol{r}, \boldsymbol{b}, y) - N_F^2(\boldsymbol{r}, \boldsymbol{b}, y)$$

$$\Rightarrow \quad N_A(\boldsymbol{r}, \boldsymbol{b}, y_0) = 1 - e^{-\frac{1}{4}\boldsymbol{r}^2 Q_s^2(y_0)}$$

Replacing $N_F(y_0)$ by $N_F(y)$ accounts for the low-x evolution of the cross section.

$N_F(y)$ satisfies the BK equation.

Numerical calculations

$$R_{A_1 A_2} = \frac{\int_{\mathcal{S}} d^2b \frac{d\sigma_{A_1 A_2 \to J/\psi X}}{dy\, d^2b}}{A_1\, A_2\, \frac{d\sigma_{pp\to J/\psi X}}{dy}}$$

The production mechanism in pp is not known, so consider the simplest one-parameter model:

$$\frac{d\sigma_{pp\to J/\psi X}}{dy} = C\, \frac{d\sigma_{AA\to J/\psi X}}{dy}\bigg|_{A=1}$$

N_F is parameterized with DHJ or bCGC models.

DHJ model

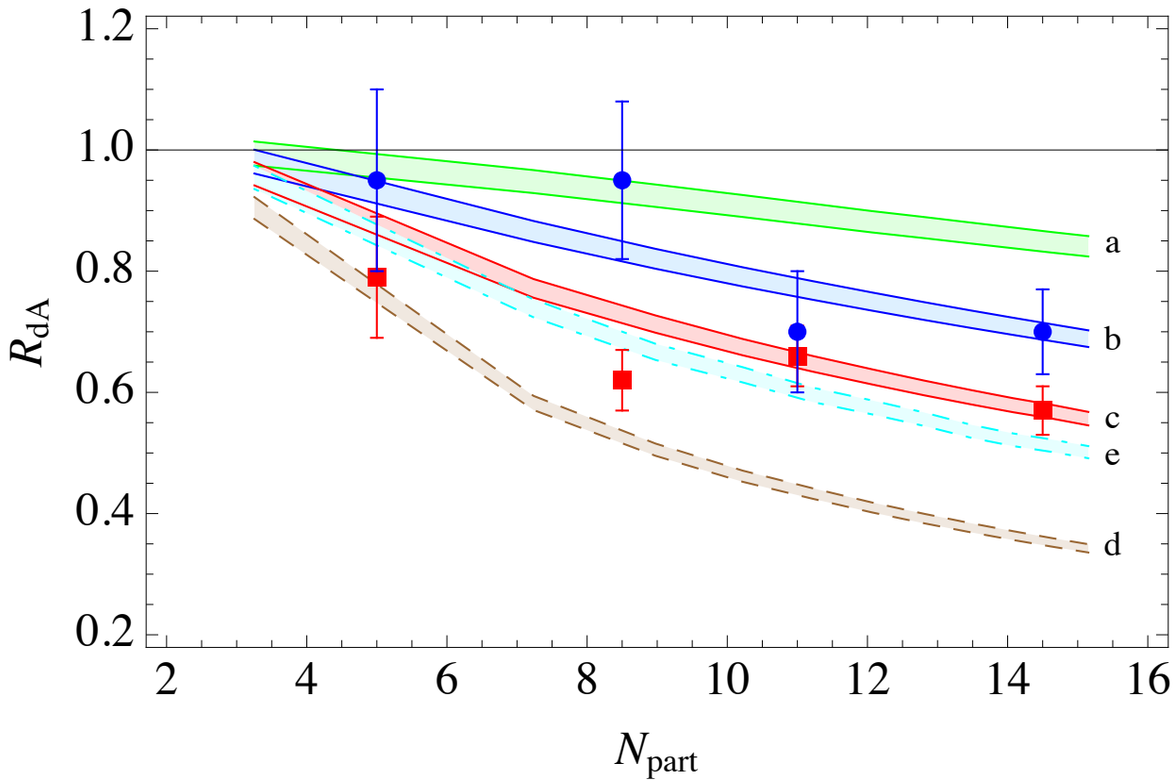

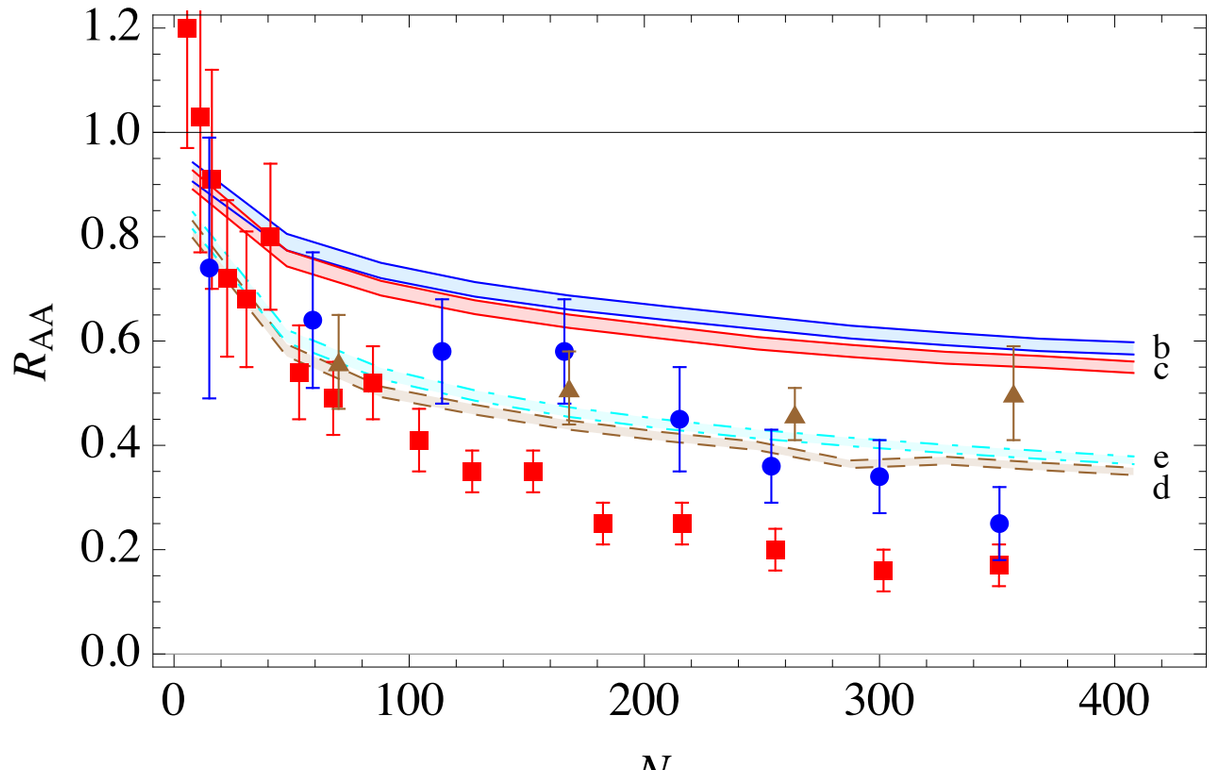

FIG. 3: Nuclear modification factor vs $N_{\rm part}$ in (a) dAu and (b) AA collisions using the DHJ model [13]. Band 'a' (green) represents rapidity $y = -1.7$ at $\sqrt{s} = 200$ GeV, 'b' (blue): $y = 0$, $\sqrt{s} = 200$ GeV, 'c' (red): $y = 1.7$, $\sqrt{s} = 200$ GeV, 'd' (brown): $y = 3.25$, $\sqrt{s} = 2.76$ TeV, 'e' (cyan): $y = 0$, $\sqrt{s} = 5.5$ TeV. $m = 1.5$ GeV, $C = 1$. Experimental data [16–19] is represented by (blue) circles in 'b', by (red) squares in 'c' and by (brown) triangles in 'd'. (Color online).

Reasonable agreement with dA and AA at LHC, undershooting of AA at RHIC

bCGC model

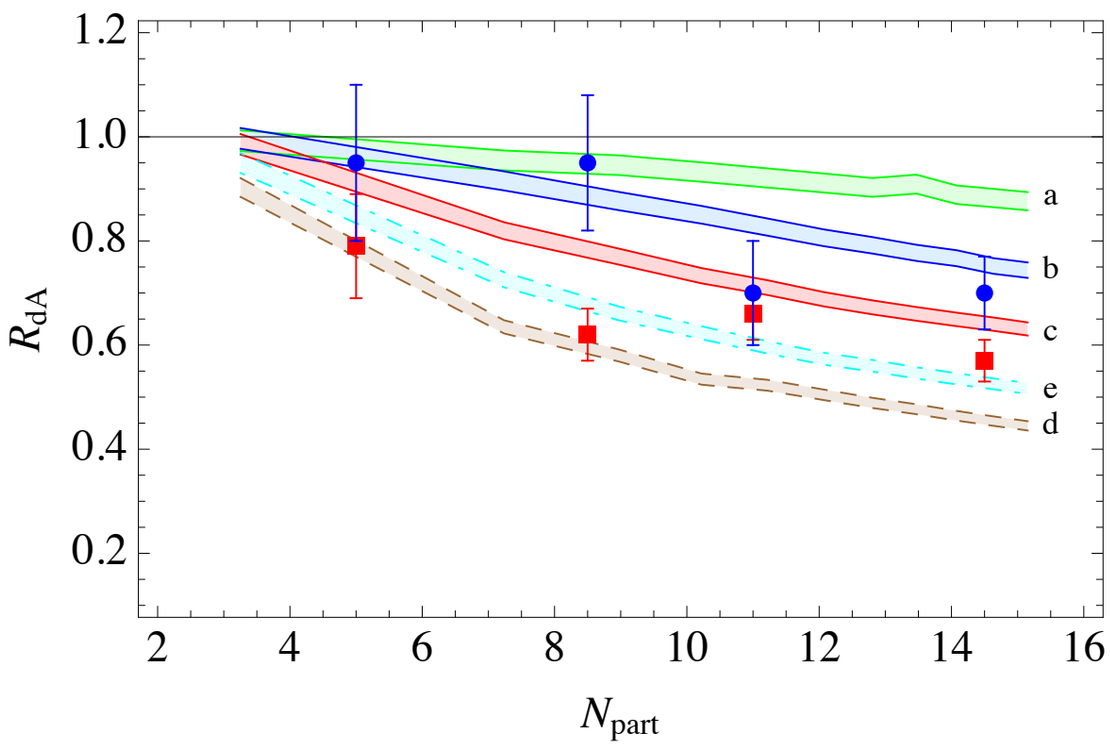

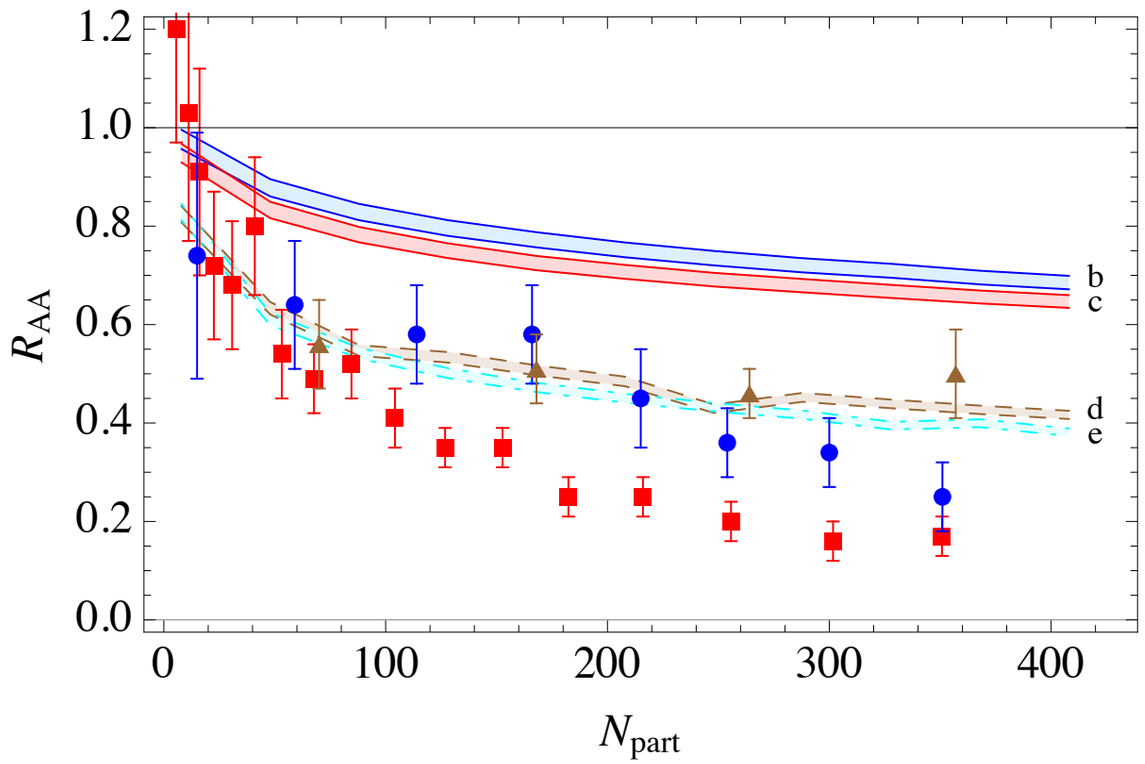

FIG. 3: Nuclear modification factor vs $N_{\rm part}$ in (a) dAu and (b) AA collisions using the DHJ model [13]. Band 'a' (green) represents rapidity $y = -1.7$ at $\sqrt{s} = 200$ GeV, 'b' (blue): $y = 0$, $\sqrt{s} = 200$ GeV, 'c' (red): $y = 1.7$, $\sqrt{s} = 200$ GeV, 'd' (brown): $y = 3.25$, $\sqrt{s} = 2.76$ TeV, 'e' (cyan): $y = 0$, $\sqrt{s} = 5.5$ TeV. $m = 1.5$ GeV, $C = 1$. Experimental data [16–19] is represented by (blue) circles in 'b', by (red) squares in 'c' and by (brown) triangles in 'd'. (Color online).

Reasonable agreement with dA and AA at LHC, undershooting of AA at RHIC

Conclusions I

•The cold nuclear matter effects alone cannot provide neither quantitative nor even a qualitative description of the AA data. Additional mechanisms beyond the initial state effects are required to explain the experimental data.

- NMF is well described with C=1 ⇒

evidence that J/ψ production mechanism in pp collisions is similar to that in pA implying that it is perhaps dominated by the higher twist effects.

pT - spectrum

To obtain the p_T spectrum we have to keep the logarithms that were neglected in the GBW model, e.g. instead of $\boldsymbol{r}\cdot\boldsymbol{r}'$ we have

$$J(\boldsymbol{r},\boldsymbol{r}',\boldsymbol{\Delta}) = \int \frac{d\ell^2}{\ell^4} e^{-i\boldsymbol{\Delta}\cdot\boldsymbol{\ell}} \left(e^{i\frac{1}{2}(\boldsymbol{r}-\boldsymbol{r}')\cdot\boldsymbol{\ell}} + e^{-i\frac{1}{2}(\boldsymbol{r}-\boldsymbol{r}')\cdot\boldsymbol{\ell}} - e^{-i\frac{1}{2}(\boldsymbol{r}+\boldsymbol{r}')\cdot\boldsymbol{\ell}} - e^{i\frac{1}{2}(\boldsymbol{r}+\boldsymbol{r}')\cdot\boldsymbol{\ell}} \right)$$

$$= \frac{2\pi}{4}\left[-\left(\frac{1}{2}(\boldsymbol{r}-\boldsymbol{r}')-\boldsymbol{\Delta}\right)^2 \ln\frac{1}{\mu|\frac{1}{2}(\boldsymbol{r}-\boldsymbol{r}')-\boldsymbol{\Delta}|} \right.$$

$$-\left(\frac{1}{2}(\boldsymbol{r}-\boldsymbol{r}')+\boldsymbol{\Delta}\right)^2 \ln\frac{1}{\mu|\frac{1}{2}(\boldsymbol{r}-\boldsymbol{r}')+\boldsymbol{\Delta}|}$$

$$+\left(\frac{1}{2}(\boldsymbol{r}+\boldsymbol{r}')+\boldsymbol{\Delta}\right)^2 \ln\frac{1}{\mu|\frac{1}{2}(\boldsymbol{r}+\boldsymbol{r}')+\boldsymbol{\Delta}|}$$

$$\left. +\left(\frac{1}{2}(\boldsymbol{r}+\boldsymbol{r}')-\boldsymbol{\Delta}\right)^2 \ln\frac{1}{\mu|\frac{1}{2}(\boldsymbol{r}+\boldsymbol{r}')-\boldsymbol{\Delta}|} \right].$$

We assume that the short distance effects can be approximately factored out: $J(\boldsymbol{r},\boldsymbol{r}',\boldsymbol{\Delta}) \approx \underbrace{\boldsymbol{r}\cdot\boldsymbol{r}'}\,\underbrace{F(\Delta)}$

projects onto 1^{--} state from pp

We are interested to calculate the nuclear modification of p_T spectrum in pA collisions. So we use the pp spectrum as input.

$$F(\Delta) = \frac{1}{\sigma_{pp\to J/\psi X}} \int \frac{d\sigma_{pp\to J/\psi X}(p_\perp)}{d^2p_\perp} e^{-i\boldsymbol{p}\cdot\boldsymbol{\Delta}} d^2p_\perp$$

Fit of experimental data: $\dfrac{d\sigma_{pp\to J/\psi X}}{\sigma_{pp}\, d^2p_\perp} = \mathcal{N}\left(1+\dfrac{p_\perp^2}{p_0^2}\right)^{-6}$

Its Fourier image: $F(\Delta) = \dfrac{(p_0\Delta)^5}{384} K_5(p_0\Delta)$

Going through the same steps as for the total cross section we got the final expression for the spectrum:

$$\frac{d\sigma_{A_1A_2\to J/\psi X}}{d^2p_\perp dy d^2B_1 d^2B_2} = \frac{d\sigma_{A_1A_2\to J/\psi X}}{dy d^2B_1 d^2B_2} \frac{1}{Q_{s1}^2+Q_{s2}^2} \int \frac{d^2\Delta}{(2\pi)^2} e^{i\boldsymbol{\Delta}\cdot\boldsymbol{p}} F(\Delta) \frac{4}{\Delta^2} \left(1-e^{-\frac{1}{4}(Q_{s1}^2+Q_{s2}^2)\Delta^2}\right)$$

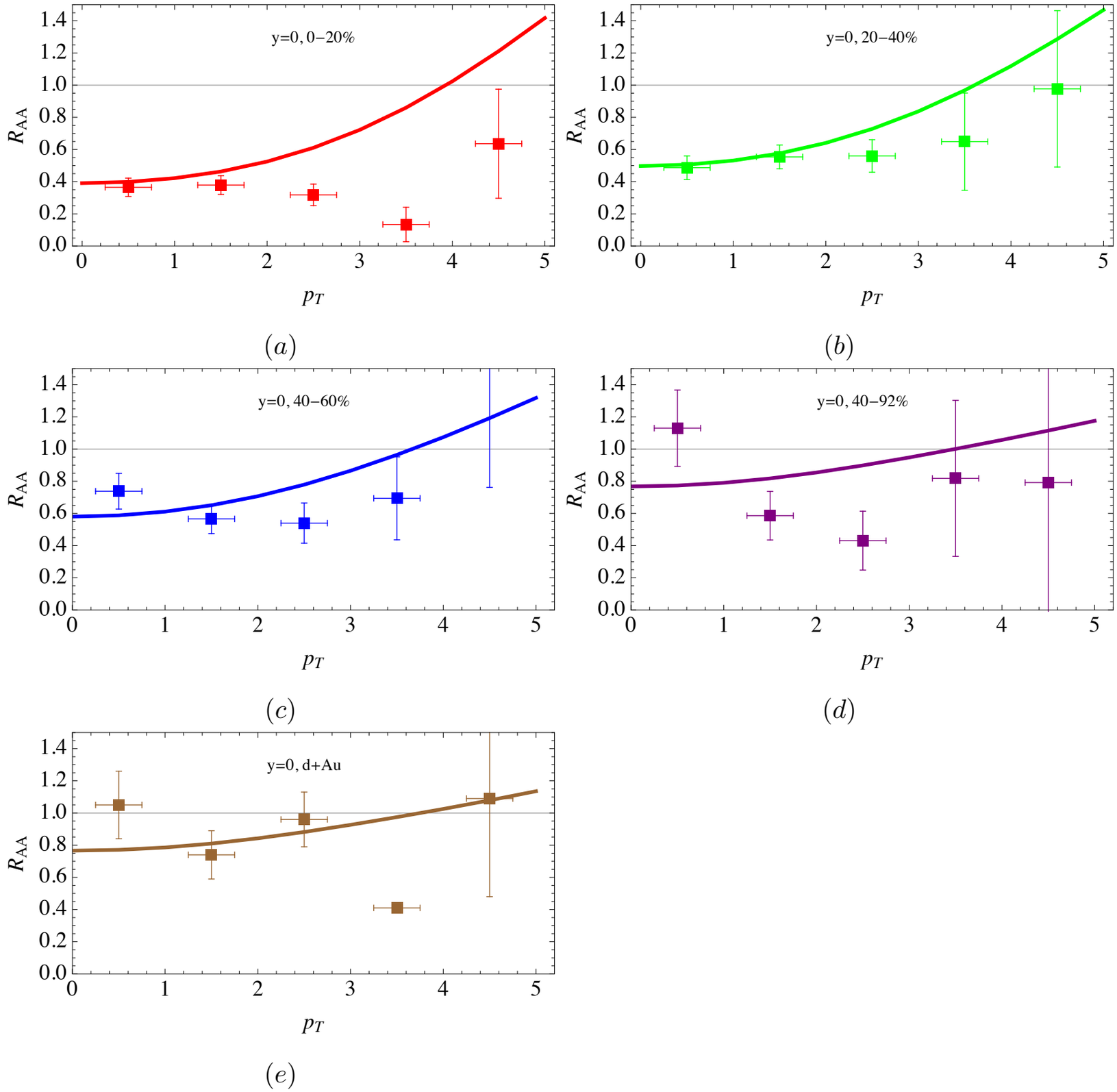

FIG. 4: (Color online). Nuclear modification factor for J/ψ's vs $p_\perp$ in GeV at $\sqrt{s} = 200$ GeV, $y = 0$ in $AuAu$ for centralities (a) 0-20%, (b) 20-40%, (c) 40-60%, (d) 60-92% and in (e) minbias dAu. Data is from [32, 33].

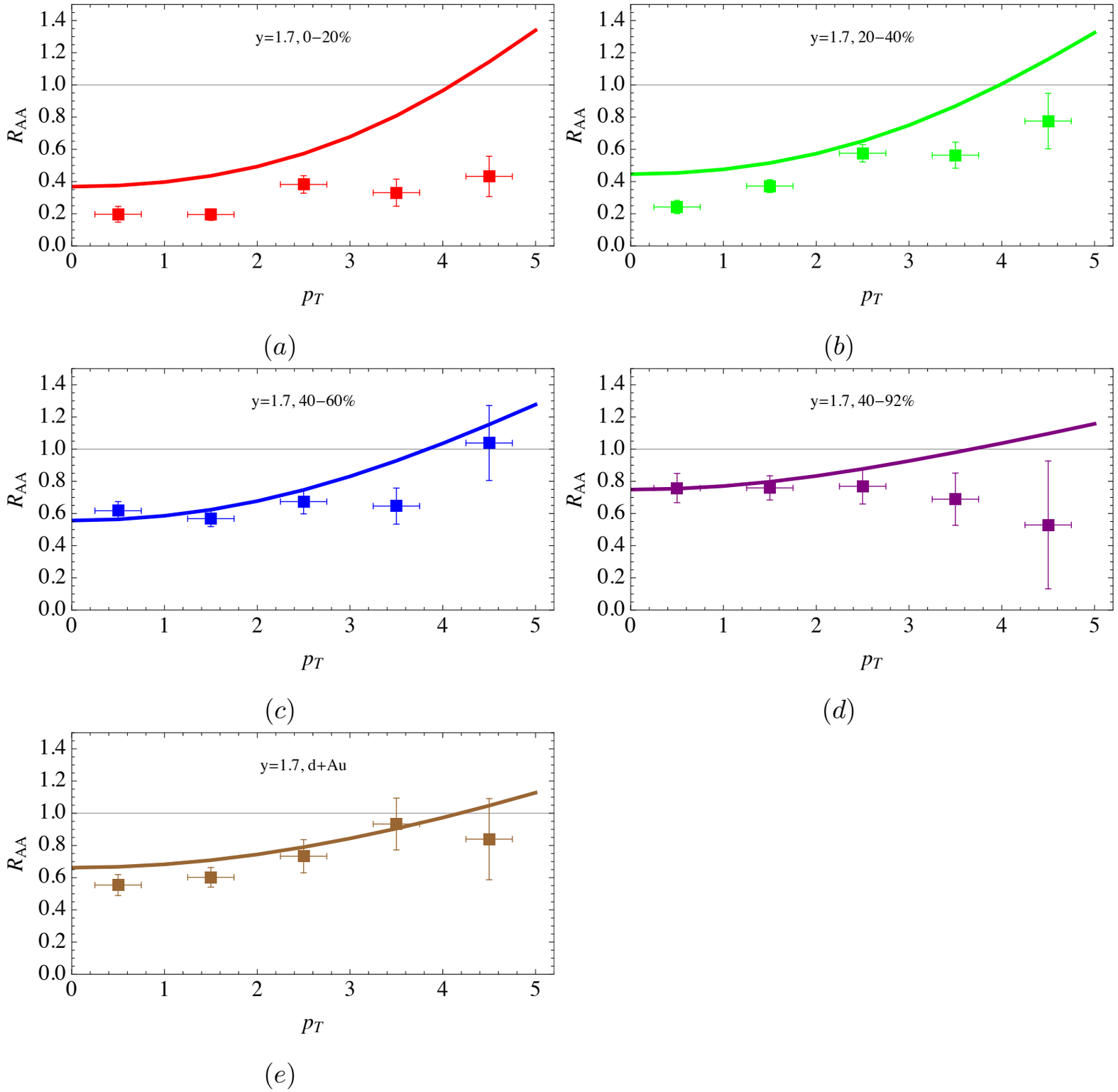

FIG. 5: (Color online). Nuclear modification factor for J/ψ's vs $p_\perp$ in GeV at $\sqrt{s} = 200$ GeV, $y = 1.7$ in $AuAu$ for centralities (a) 0-20%, (b) 20-40%, (c) 40-60%, (d) 60-92% and in (e) minbias dAu. Data is from [32, 33].

Preliminary PHENIX

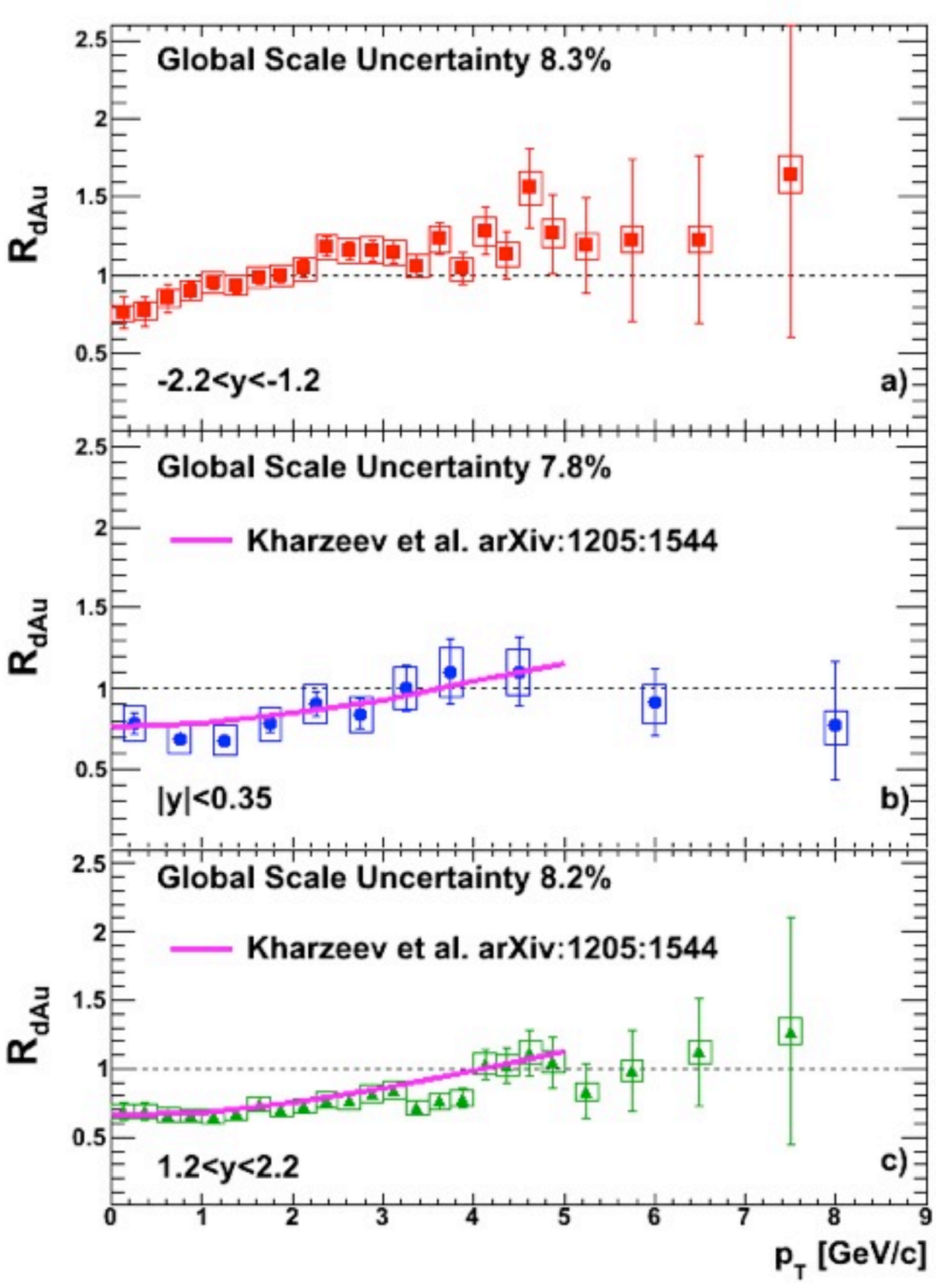

Predictions for LHC

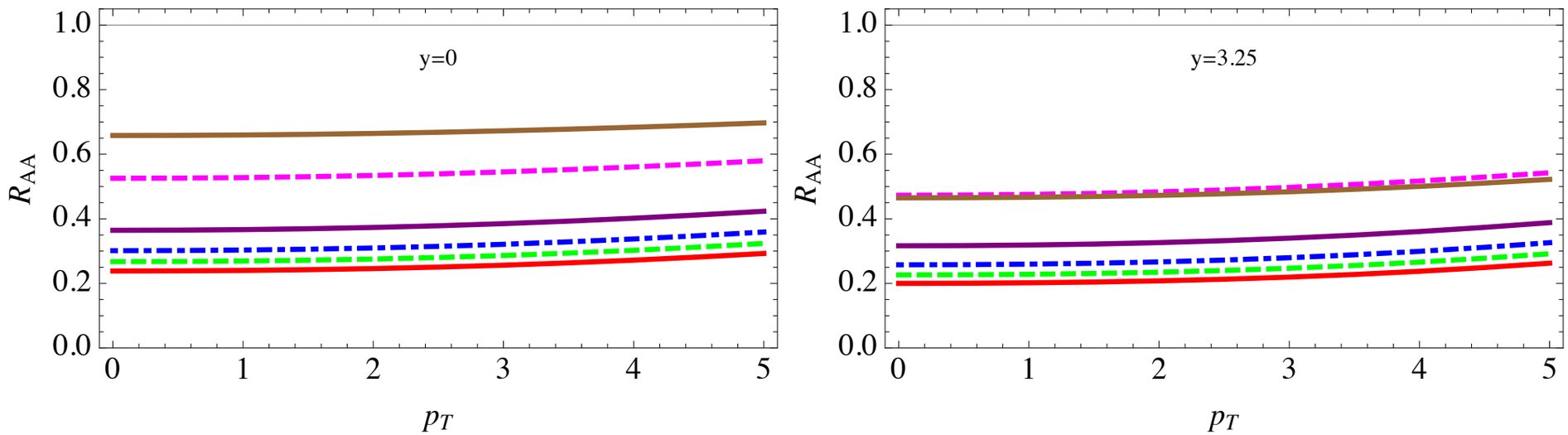

(a) (b)

FIG. 6: (Color online). Nuclear modification factor for J/ψ's vs $p_\perp$ in GeV at $\sqrt{s} = 7$ TeV in $PbPb$ for rapidities (a) $y = 0$ and (b) $y = 3.25$. Each line corresponds to a different centrality bin; from bottom to top: 0-10% (solid red), 10-20% (dashed green), 20-30% (dash-dotted blue), 30-50% (solid purple), 50-80% (dashed magenta) and in minbias pPb (solid brown).

Conclusions II

• J/ψ suppression that originates from the initial state (cold nuclear matter) effects increases at the LHC energies compared to RHIC. Meanwhile, the experimental data on AA collisions indicate that J/ψ's are suppressed less at LHC than at RHIC.

• The hot (or any other) non-CGC effect increases with p_T :

✓ Possible explanation: dissociation of J/ψ in magnetic field.

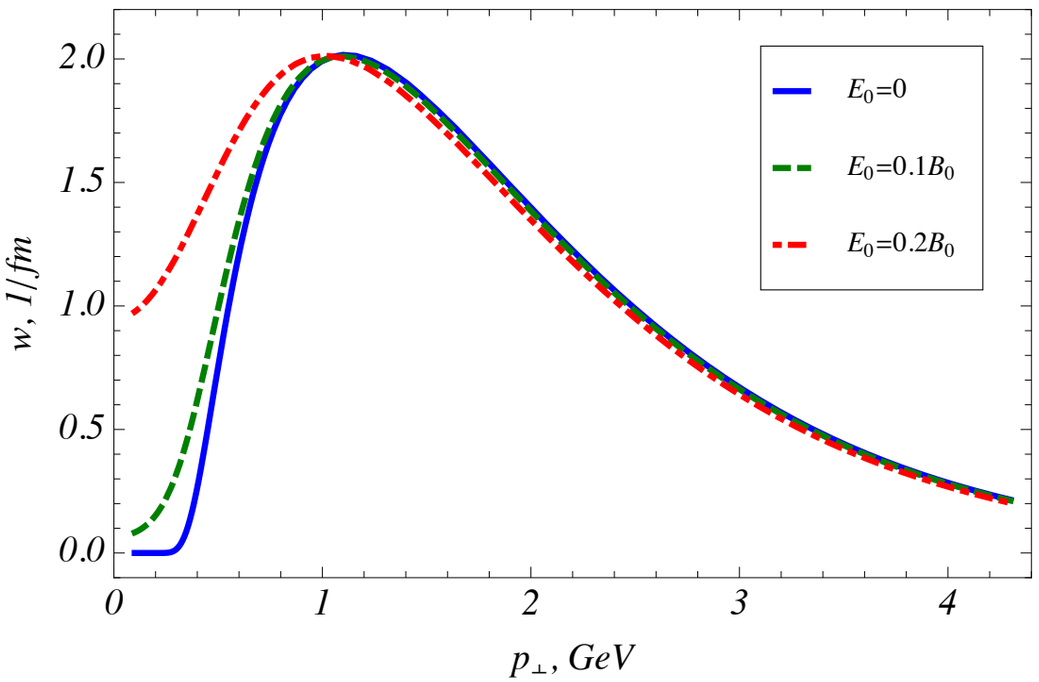

KT (2010)

Open charm

Kovchegov, KT (2006)

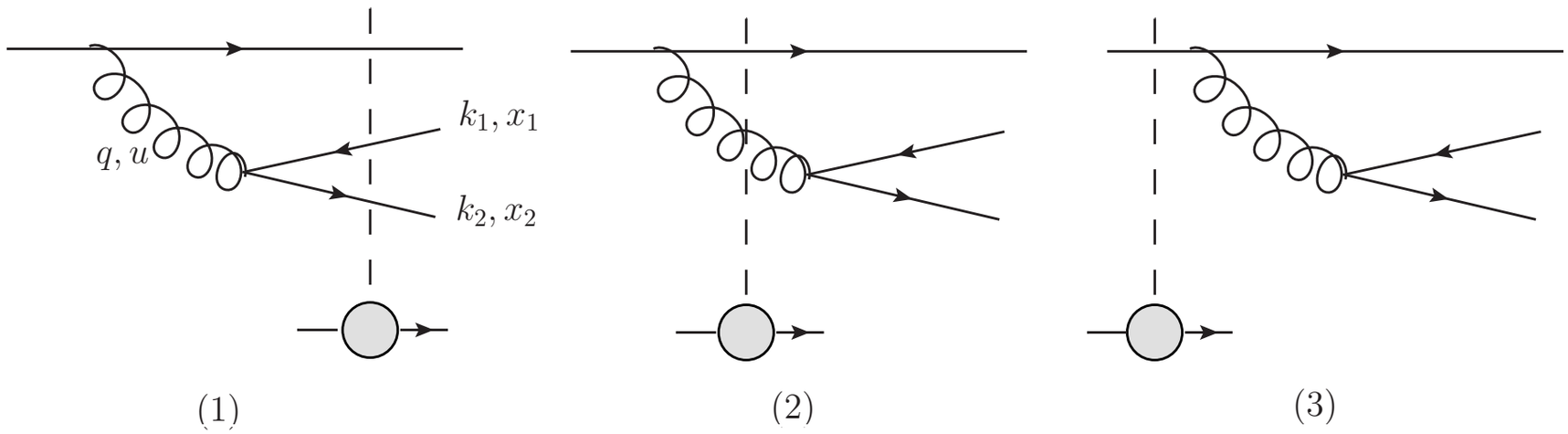

Usual approximation is to neglect the contribution of valence quark, which is true if $q \ll 2m$

KT (2005,2007)

$$\frac{d\sigma^{q_v \to q\bar{q}X}_{\rm fact}}{d^2\ell\, d^2q\, dy\, dz\, d^2b} = \frac{1}{(2\pi)^4} C_F \left(\frac{\alpha_s}{\pi}\right)^2 \frac{m^2}{q^2} \int d^2r d^2r'\, e^{-i\boldsymbol{\ell}\cdot(\boldsymbol{r}-\boldsymbol{r}')}$$
$$\times \left\{ K_1(rm) K_1(r'm) \frac{\boldsymbol{r}\cdot\boldsymbol{r}'}{rr'} [(1-z)^2 + z^2] + K_0(rm) K_0(r'm) \right\}$$
$$\times \Big\{ S_F\big((1-z)(\boldsymbol{r}-\boldsymbol{r}')\big) S_F\big(z(\boldsymbol{r}-\boldsymbol{r}')\big) + 1$$
$$- S_F\big((1-z)\boldsymbol{r}\big) S_F(z\boldsymbol{r}) - S_F\big((1-z)\boldsymbol{r}'\big) S_F(z\boldsymbol{r}') \Big\}.$$

$$S_F = 1 - N$$

Proton factorization limit

Kopeliovich, Tarasov (2002)

KT (2005)

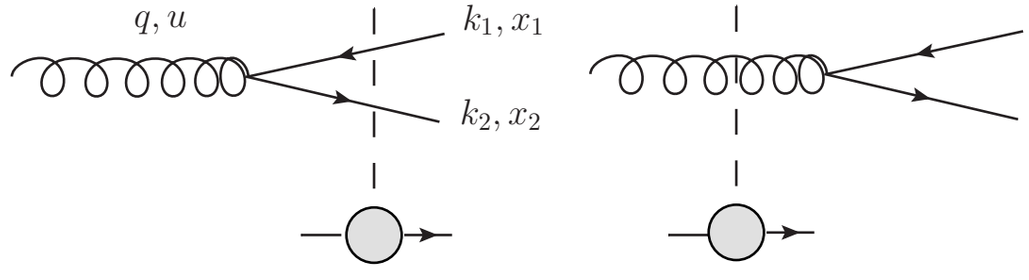

$$x_p G(x_p, Q^2) = \int^{Q^2} \varphi(x_p, q^2)\, dq^2 \qquad \varphi(x_p, q^2) = \frac{\alpha_s C_F}{\pi\, q^2}$$

Unintegrated gluon distribution factors out ☞

collinear factorization on the proton side.

In the chiral limit $$\phi^{g\to q\bar{q}}(\boldsymbol{r}, \boldsymbol{r}', z) = \frac{2g^2}{(2\pi)^2}\delta(\boldsymbol{u})\delta(\boldsymbol{u}')\frac{\boldsymbol{r}\cdot\boldsymbol{r}'}{r^2 r'^2} P_{qg}(z)$$

$$P_{qg}(z) = \frac{1}{2}[(1-z)^2 + z^2]$$

Open charm

It is important to know the cold-nuclear matter effects on open charm!

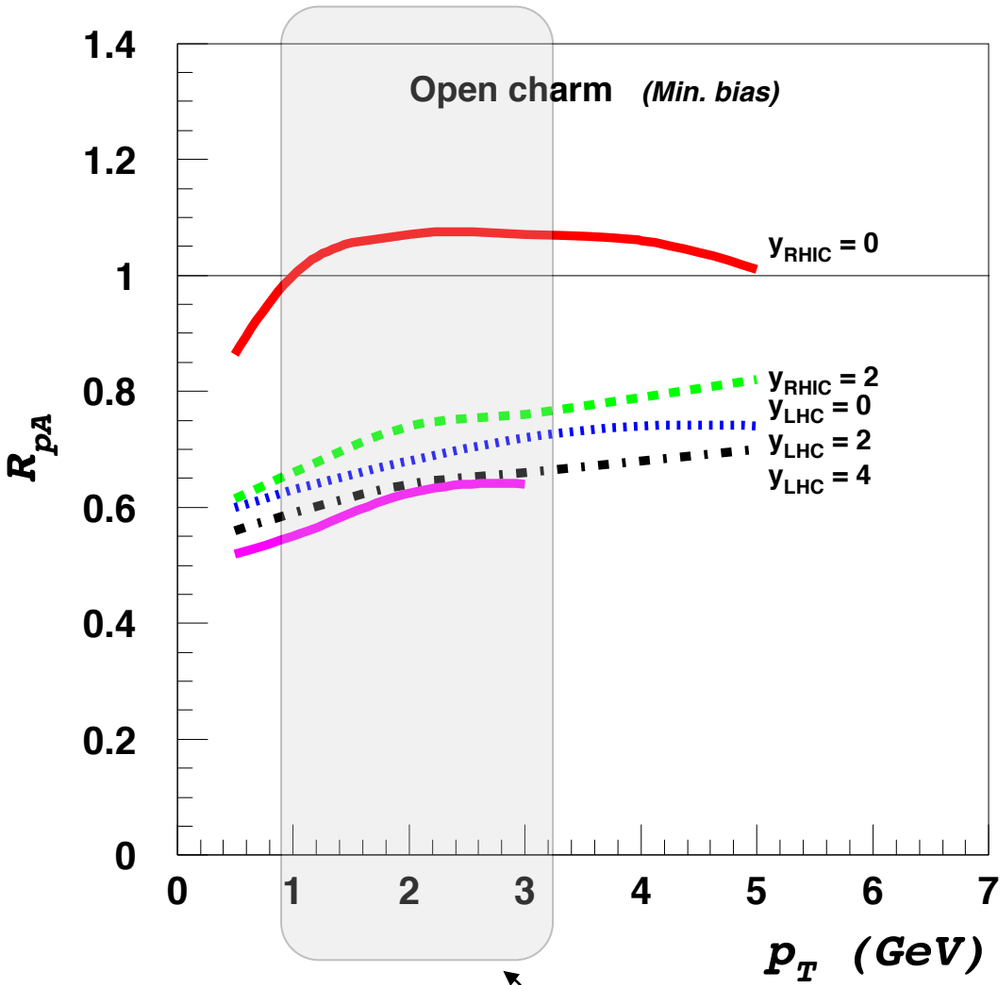

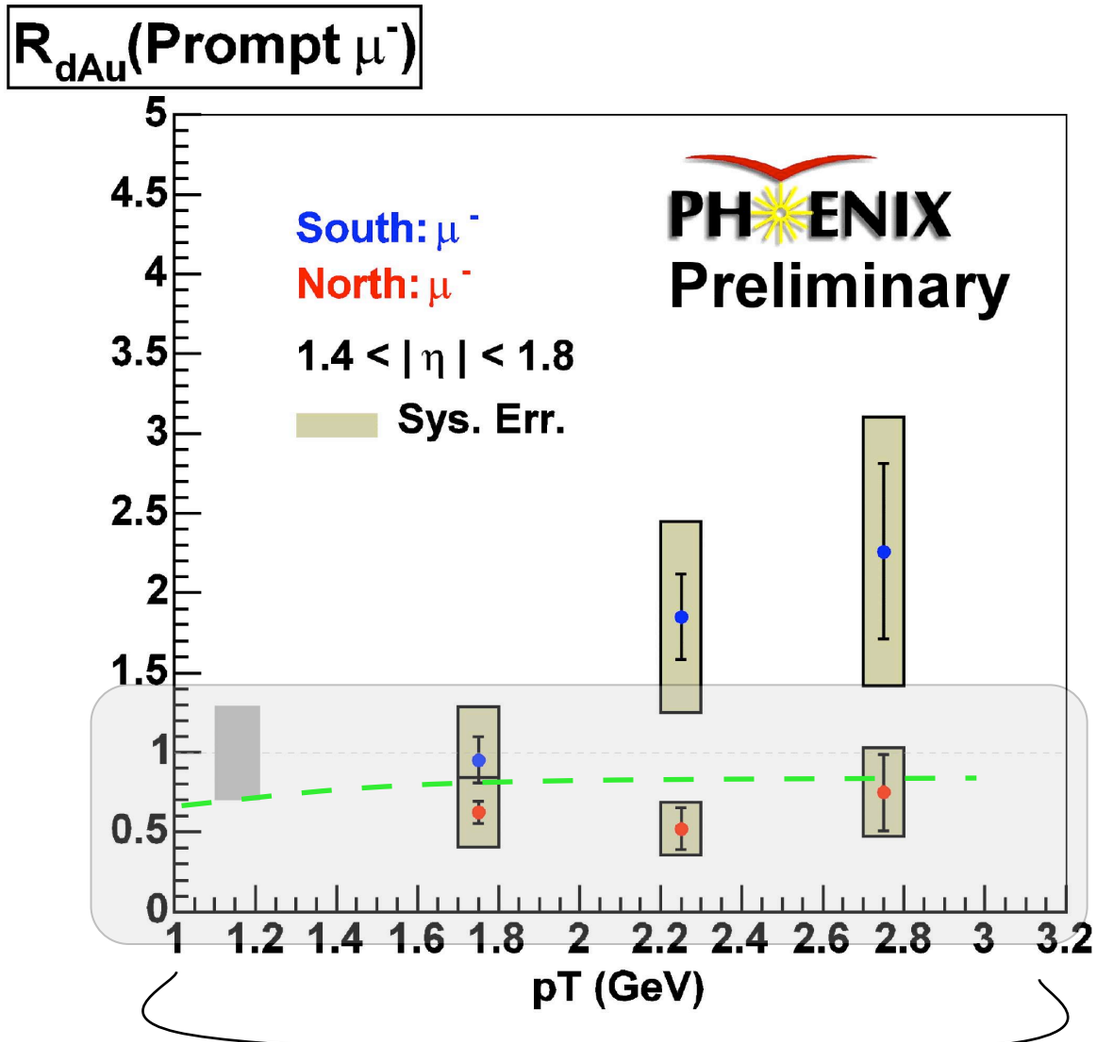

KT, 2007

Suppression of heavy quarks in forward direction

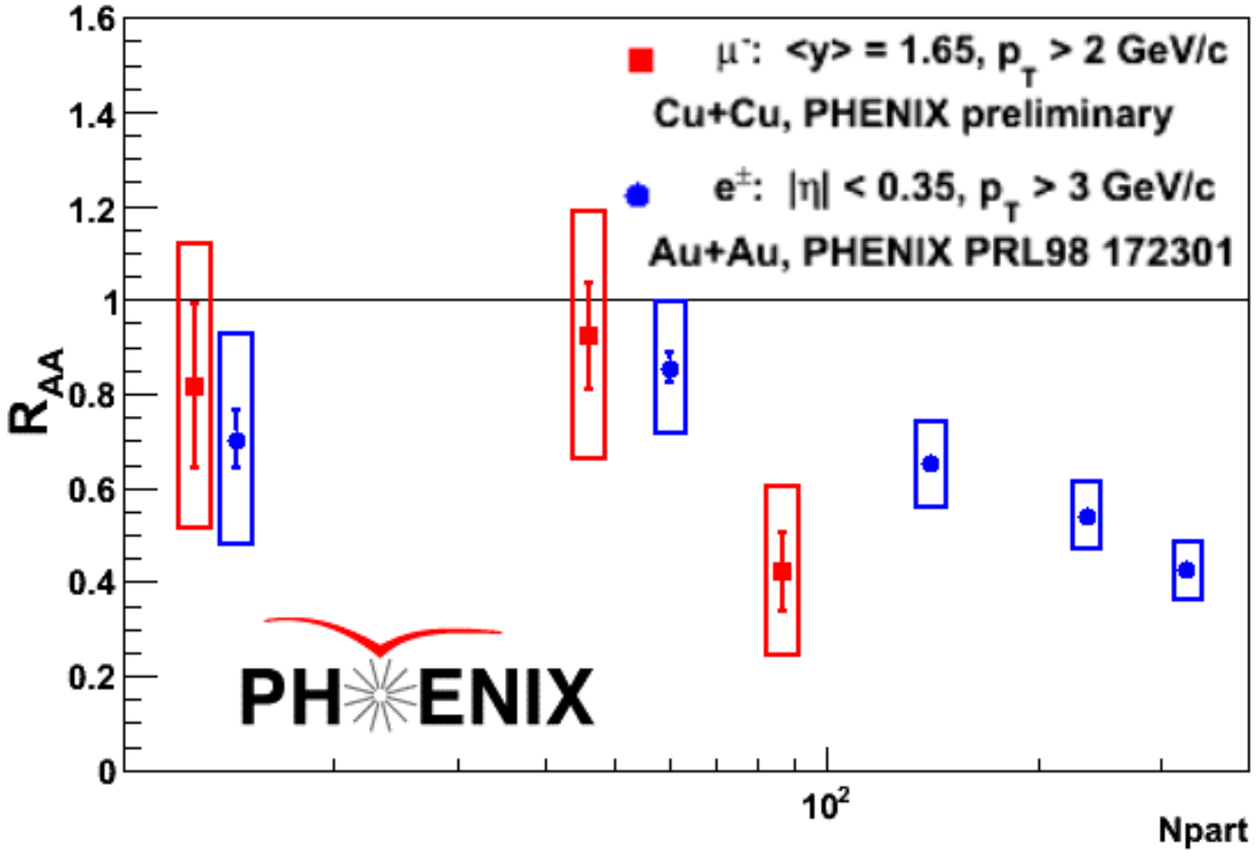

Similar effect for heavy-ion collisions. The overall suppression is a combination of cold and hot nuclear matter effects.

c-quark: proton factorization

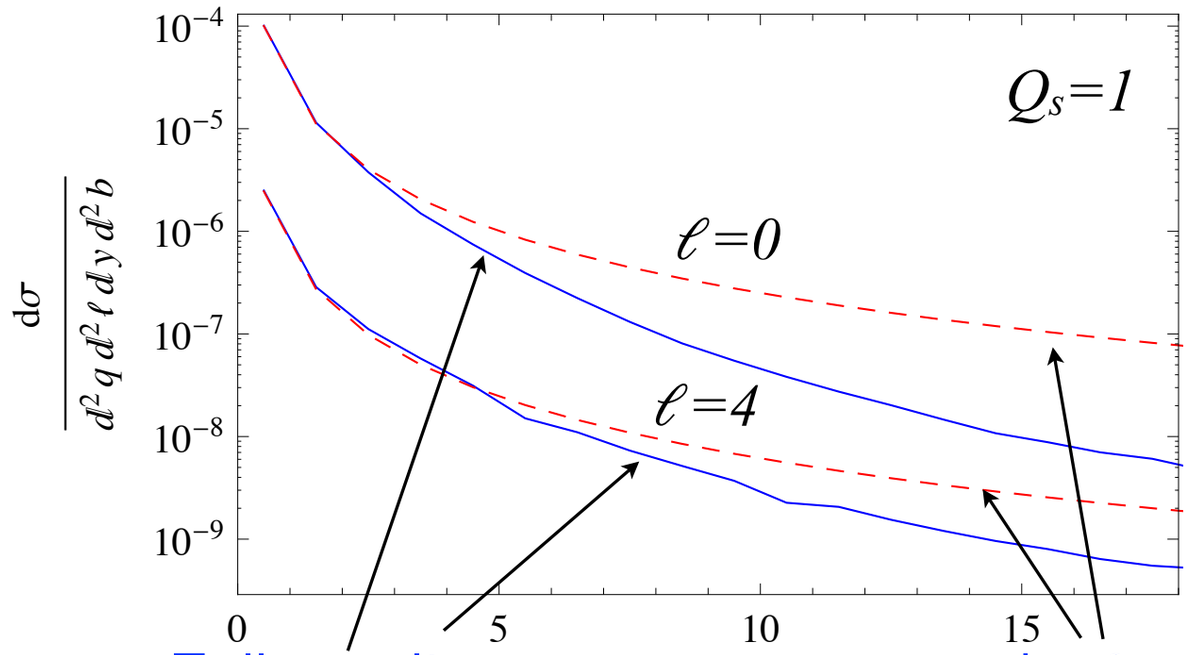

Full result

k_T-factorization of proton

$\ell=4, Q_s=1$

c-quark: nucleus factorization

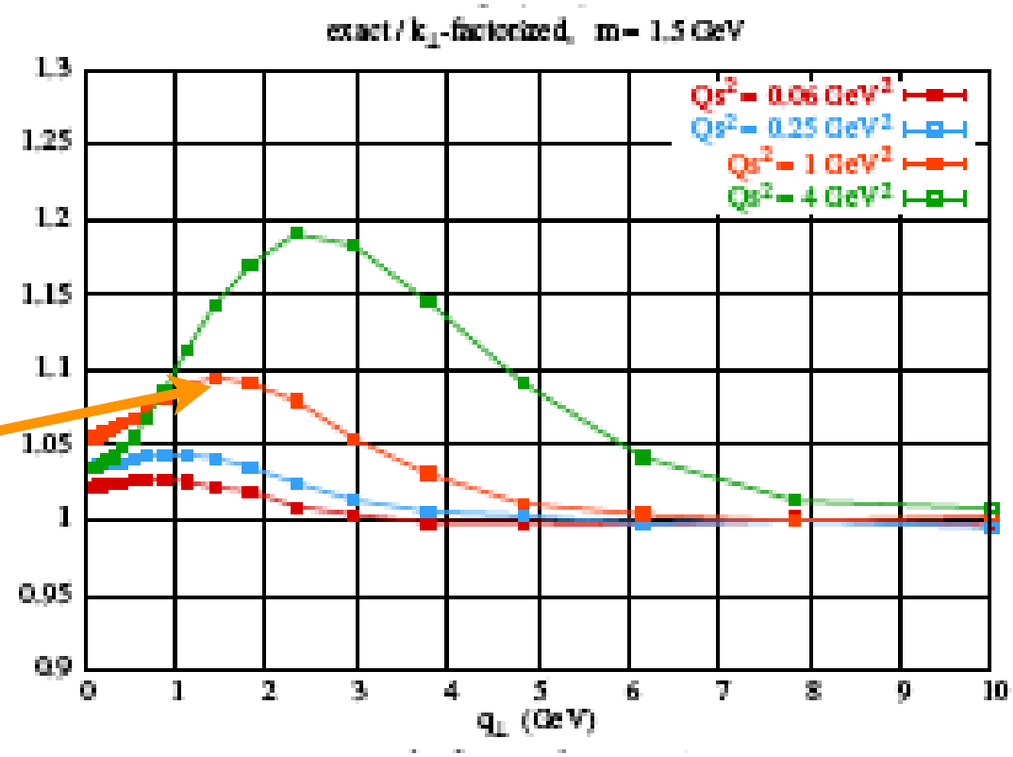

RHIC

Fujii, Gelis, Venugopalan

Where is transition to hard pQCD?

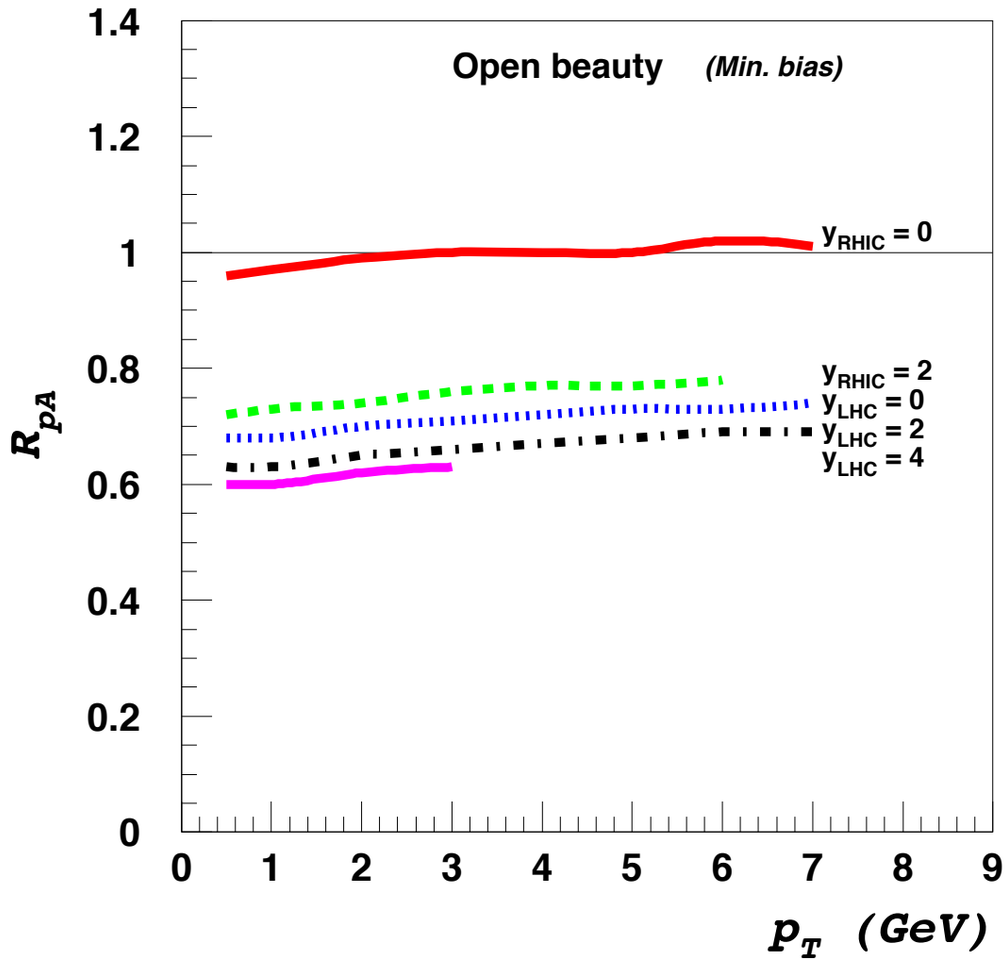

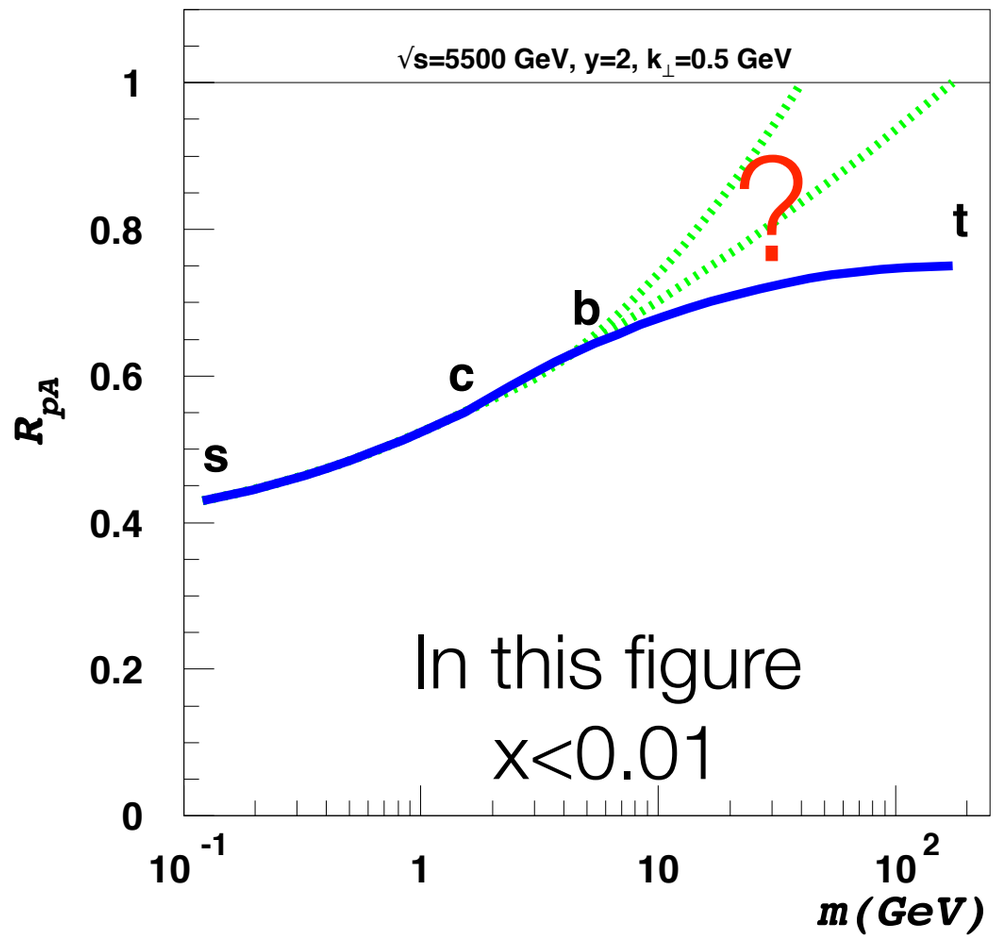

$$\alpha_s \log \frac{Q_s^2}{\Lambda_{\rm QCD}} \quad \overset{?}{\Leftrightarrow} \quad \alpha_s \log \frac{Q^2}{Q_s^2}$$

Summary

• Cold nuclear matter (CNM) effects on J/ψ are now under a good theoretical control, especially at LHC energies.

• CNM effects increase with energy and rapidity and decrease with p_T.

• The difference between the NMF due to CNM and the one experimentally observed may be due to QGP or magnetic field. Its energy and p_T dependence is puzzling.